



# TECH BRIEFS

NATIONAL AERONAUTICS AND SPACE ADMINISTRATION

-  **Technology Focus**
-  **Electronics/Computers**
-  **Software**
-  **Materials**
-  **Mechanics/Machinery**
-  **Manufacturing**
-  **Bio-Medical**
-  **Physical Sciences**
-  **Information Sciences**
-  **Books and Reports**



## INTRODUCTION

Tech Briefs are short announcements of innovations originating from research and development activities of the National Aeronautics and Space Administration. They emphasize information considered likely to be transferable across industrial, regional, or disciplinary lines and are issued to encourage commercial application.

### Availability of NASA Tech Briefs and TSPs

Requests for individual Tech Briefs or for Technical Support Packages (TSPs) announced herein should be addressed to

#### National Technology Transfer Center

Telephone No. (800) 678-6882 or via World Wide Web at [www2.nttc.edu/leads/](http://www2.nttc.edu/leads/)

Please reference the control numbers appearing at the end of each Tech Brief. Information on NASA's Innovative Partnerships Program (IPP), its documents, and services is also available at the same facility or on the World Wide Web at <http://ipp.nasa.gov>.

Innovative Partnerships Offices are located at NASA field centers to provide technology-transfer access to industrial users. Inquiries can be made by contacting NASA field centers listed below.

## NASA Field Centers and Program Offices

#### Ames Research Center

Lisa L. Lockyer  
(650) 604-1754  
[lisa.l.lockyer@nasa.gov](mailto:lisa.l.lockyer@nasa.gov)

#### Dryden Flight Research Center

Gregory Poteat  
(661) 276-3872  
[greg.poteat@dfrc.nasa.gov](mailto:greg.poteat@dfrc.nasa.gov)

#### Glenn Research Center

Kathy Needham  
(216) 433-2802  
[kathleen.k.needham@nasa.gov](mailto:kathleen.k.needham@nasa.gov)

#### Goddard Space Flight Center

Nona Cheeks  
(301) 286-5810  
[nona.k.cheeks@nasa.gov](mailto:nona.k.cheeks@nasa.gov)

#### Jet Propulsion Laboratory

Ken Wolfenbarger  
(818) 354-3821  
[james.k.wolfenbarger@jpl.nasa.gov](mailto:james.k.wolfenbarger@jpl.nasa.gov)

#### Johnson Space Center

Michele Brekke  
(281) 483-4614  
[michele.a.brekke@nasa.gov](mailto:michele.a.brekke@nasa.gov)

#### Kennedy Space Center

David R. Makufka  
(321) 867-6227  
[david.r.makufka@nasa.gov](mailto:david.r.makufka@nasa.gov)

#### Langley Research Center

Martin Waszak  
(757) 864-4015  
[martin.r.waszak@nasa.gov](mailto:martin.r.waszak@nasa.gov)

#### Marshall Space Flight Center

Jim Dowdy  
(256) 544-7604  
[jim.dowdy@msfc.nasa.gov](mailto:jim.dowdy@msfc.nasa.gov)

#### Stennis Space Center

John Bailey  
(228) 688-1660  
[john.w.bailey@nasa.gov](mailto:john.w.bailey@nasa.gov)

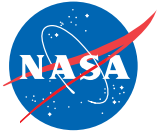
#### Carl Ray, Program Executive

Small Business Innovation  
Research (SBIR) & Small  
Business Technology  
Transfer (STTR) Programs  
(202) 358-4652  
[carl.g.ray@nasa.gov](mailto:carl.g.ray@nasa.gov)

#### Doug Comstock, Director

Innovative Partnerships  
Program Office  
(202) 358-2560  
[doug.comstock@nasa.gov](mailto:doug.comstock@nasa.gov)





# TECH BRIEFS

NATIONAL AERONAUTICS AND SPACE ADMINISTRATION



## 5 Technology Focus: Sensors

- 5 Customizable Digital Receivers for Radar
- 6 Two-Camera Acquisition and Tracking of a Flying Target
- 7 Visual Data Analysis for Satellites
- 7 A Data Type for Efficient Representation of Other Data Types
- 8 Hand-Held Ultrasonic Instrument for Reading Matrix Symbols



## 11 Electronics/Computers

- 11 Broadband Microstrip-to-Coplanar Strip Double-Y Balun
- 12 A Topographical Lidar System for Terrain-Relative Navigation
- 12 Programmable Low-Voltage Circuit Breaker and Tester
- 13 Electronic Switch Arrays for Managing Microbattery Arrays
- 14 Lower-Dark-Current, Higher-Blue-Response CMOS Imagers



## 17 Manufacturing & Prototyping

- 17 Fabricating Large-Area Sheets of Single-Layer Graphene by CVD



## 19 Software

- 19 Support for Diagnosis of Custom Computer Hardware
- 19 Providing Goal-Based Autonomy for Commanding a Spacecraft
- 19 Dynamic Method for Identifying Collected Sample Mass
- 19 Optimal Planning and Problem-Solving
- 20 Attitude-Control Algorithm for Minimizing Maneuver Execution Errors
- 20 Grants Document-Generation System



## 21 Materials

- 21 Heat-Storage Modules Containing  $\text{LiNO}_3 \cdot 3\text{H}_2\text{O}$  and Graphite Foam
- 21 Precipitation-Strengthened, High-Temperature, High-Force Shape Memory Alloys



## 23 Mechanics & Machinery

- 23 Improved Relief Valve Would Be Less Susceptible to Failure
- 24 Safety Modification of Cam-and-Groove Hose Coupling
- 24 Using Composite Materials in a Cryogenic Pump



## 27 Bio-Medical

- 27 Using Electronic Noses To Detect Tumors During Neurosurgery
- 28 Producing Newborn Synchronous Mammalian Cells



## 29 Physical Sciences

- 29 Smaller, Lower-Power Fast-Neutron Scintillation Detectors
- 29 Rotationally Vibrating Electric-Field Mill
- 30 Estimating Hardness From the USDC Tool-Bit Temperature Rise
- 31 Particle-Charge Spectrometer



## 33 Information Sciences

- 33 Automated Production of Movies on a Cluster of Computers



## 35 Books & Reports

- 35 FIDO-Class Development Rover
- 35 Tone-Based Command of Deep Space Probes Using Ground Antennas

This document was prepared under the sponsorship of the National Aeronautics and Space Administration. Neither the United States Government nor any person acting on behalf of the United States Government assumes any liability resulting from the use of the information contained in this document, or warrants that such use will be free from privately owned rights.





## Customizable Digital Receivers for Radar

These receivers are unusually compact and versatile.

NASA's Jet Propulsion Laboratory, Pasadena, California

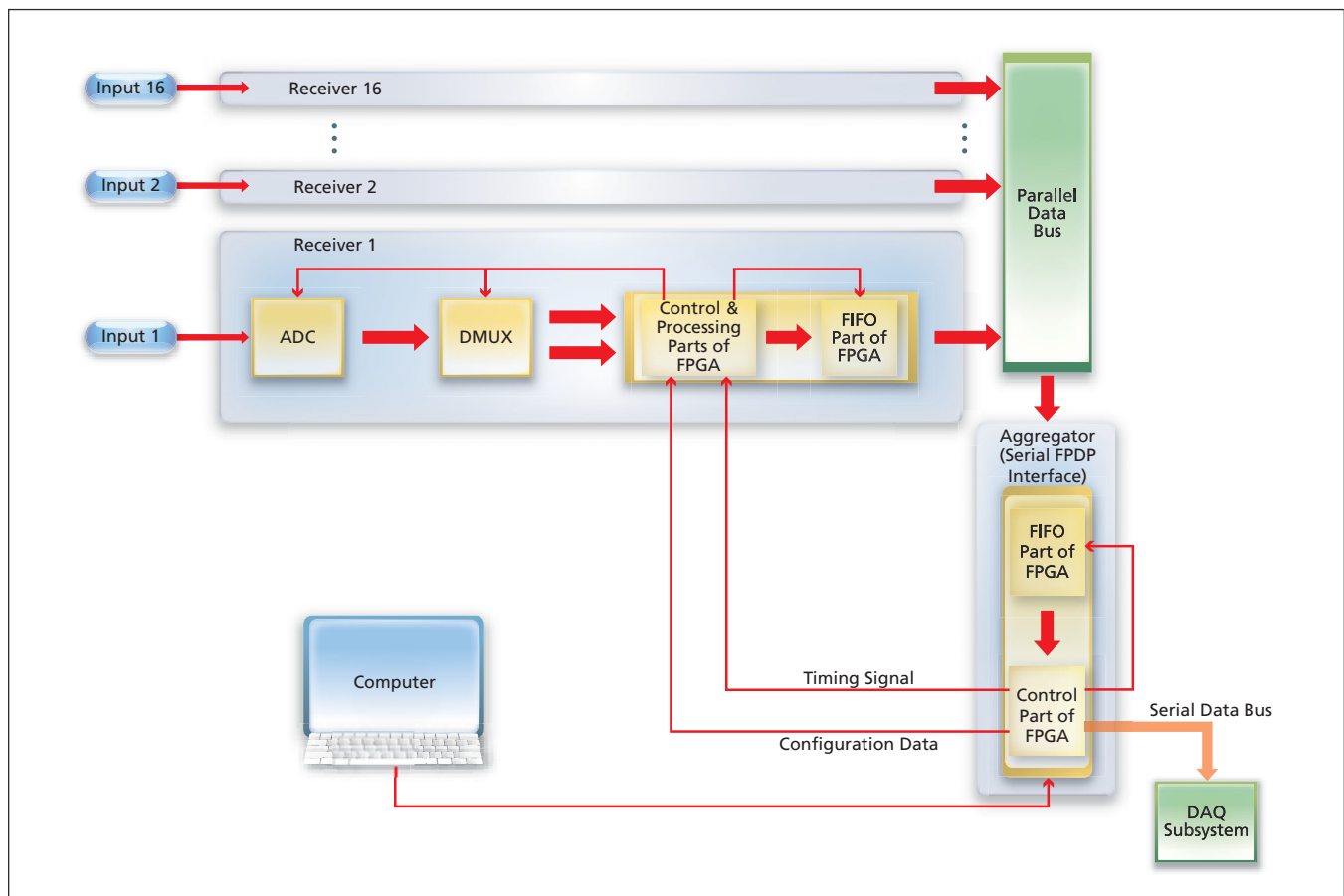
Compact, highly customizable digital receivers are being developed for the system described in "Radar Interferometer for Topographic Mapping of Glaciers and Ice Sheets" (NPO-43962), *NASA Tech Briefs*, Vol. 31, No. 7 (August 2007), page 72. In the original intended application, there is a requirement for 16 such receivers, each dedicated to, and mounted directly on, one antenna element in a 16-element array. The receivers are required to operate in unison, sampling radar returns received by the antenna elements in a digital beam-forming (DBF) mode. The design of these receivers could also be adapted to commercial radar systems. At the time of reporting the information for this article, there were no com-

mercially available digital receivers capable of satisfying all of the operational requirements and compact enough to be mounted directly on the antenna elements.

The figure depicts the overall system of which the digital receivers are parts. Each digital receiver includes an analog-to-digital converter (ADC), a demultiplexer (DMUX), and a field-programmable gate array (FPGA). The ADC effects 10-bit band-pass sampling of input signals having frequencies up to 3.5 GHz. (In the original intended application, the input signals would be intermediate-frequency signals obtained through down-conversion of signals from a radio frequency of several tens of gigahertz.) The input samples are de-

multiplexed at a user-selectable rate of 1:2 or 1:4, then buffered in part of the FPGA that functions as a first-in/first-out (FIFO) memory. Another part of the FPGA serves as a controller for the ADC, DMUX, and FIFO memory and as an interface between (1) the rest of the receiver and (2) a front-panel data port (FPDP) bus, which is an industry-standard parallel data bus that has a high-data-rate capability and multichannel configuration suitable for DBF.

Still other parts of the FPGA in each receiver perform signal-processing functions. The design exploits the capability of FPGAs to perform high-speed processing and their amenability to customization. There is ample space available within the FPGA to customize it to



Digital Receivers in an array sample and preprocess input signals from antenna elements. The receiver outputs are coupled in turn onto the parallel data bus.

implement such application-specific, real-time processes as digital filtering and data compression. To afford additional operational flexibility and to enable use of a receiver in other applications, the design also includes a provision for an additional “drop-in” circuit board containing analog amplification and filtering circuitry. Such boards, which are relatively simple and inexpensive, can be easily exchanged by the user to modify center-frequency, bandwidth, and signal-level parameters.

The digital receivers can be configured to operate in a stand-alone mode, or in a multichannel mode as needed for DBF. In the multichannel/DBF mode, the receivers are made to take turns in transmitting sampled data onto the bus. The bus port on each receiver adheres to the FPDP-II standard, which supports an aggregate data rate of 400 MB/s. While the primary role of the FPDP bus is to transmit sampled data from receivers to a data-storage unit,

the bus can also be used to transmit configuration data to the receivers. The bus also enables the receivers to communicate with one another — a capability that could be useful in some applications. Each receiver is also equipped with an RS-232 interface, through which configuration data can be communicated.

The data on the bus are aggregated and then sent to a data-acquisition (DAQ) subsystem by means of a serial FPDP interface that, like each receiver, contains an FPGA that serves partly as a FIFO memory and partly as a control unit. The DAQ subsystem stores the data onto a hard-disk array for postprocessing. In its role as a control unit, this FPGA sends timing and configuration information to each of the 16 receivers.

Although band-pass sampling is a widely applied technique, heretofore, it has been little used in radar systems. The use of band-bass sampling in the present receiver design is what makes it

possible to achieve compactness: Band-pass sampling makes it possible to feed, as input to the ADC, signals having higher frequencies than could otherwise be utilized. In so doing, band-pass sampling enables elimination of an additional down-conversion stage that would otherwise be needed, thereby reducing the design size of the receiver. This design approach also eases filtering constraints and, in so doing, reduces the required sizes of filters.

The customizability of the receiver makes it applicable to a broad range of system architectures. The capability for operation of receivers in either a stand-alone or a DBF mode enables the use of the receivers in an unprecedentedly wide variety of radar systems.

*This work was done by Delwyn Moller, Brandon Heavey, and Gregory Sadowy of Caltech for NASA's Jet Propulsion Laboratory. For more information, contact iaoffice@jpl.nasa.gov. NPO-45539*

## Two-Camera Acquisition and Tracking of a Flying Target

**An unanticipated moving target can be automatically spotted and tracked.**

*NASA's Jet Propulsion Laboratory, Pasadena, California*

A method and apparatus have been developed to solve the problem of automated acquisition and tracking, from a location on the ground, of a luminous moving target in the sky. The method involves the use of two electronic cameras: (1) a stationary camera having a wide field of view, positioned and oriented to image the entire sky; and (2) a camera that has a much narrower field of view (a few degrees wide) and is mounted on a two-axis gimbal. The wide-field-of-view stationary camera is used to initially identify the target against the background sky. So that the approximate position of the target can be determined, pixel locations on the image-detector plane in the stationary camera are calibrated with respect to azimuth and elevation. The approximate target position is used to initially aim the gimballed narrow-field-of-view camera in the approximate direction of the target. Next, the narrow-field-of-view camera locks onto the target image, and thereafter the gimbals are actuated as needed to maintain lock and thereby track the target with precision greater than that attainable by use of the stationary camera.

Figure 1 shows a prototype of the apparatus. The stationary, wide-field-of-view camera includes a fish-eye lens that projects a full view of the sky (the full 360° of azimuth and the full 90° of elevation) onto a 512×512-pixel image detector of the active-pixel-sensor type. The gimballed narrow-field-of-view camera contains a charge-coupled-device (CCD) image detector. The apparatus also includes circuitry that digitizes the image-detector outputs and a

computer that processes the image data and generates gimbal-control commands.

The stationary, wide-field-of-view camera repeatedly takes pictures of the sky. In processing of the image data for each successive frame period, the immediately preceding frame is subtracted from the current frame, so that all that remains in the image is what has changed between the two successive frames. Hence, if there is a moving luminous target, it

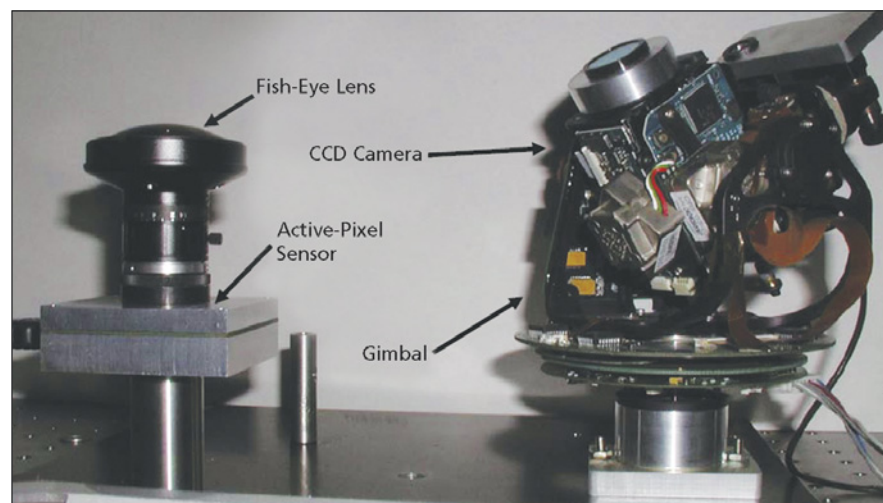


Figure 1. This **Prototype Apparatus** was built and tested, yielding the images shown in Figure 2.



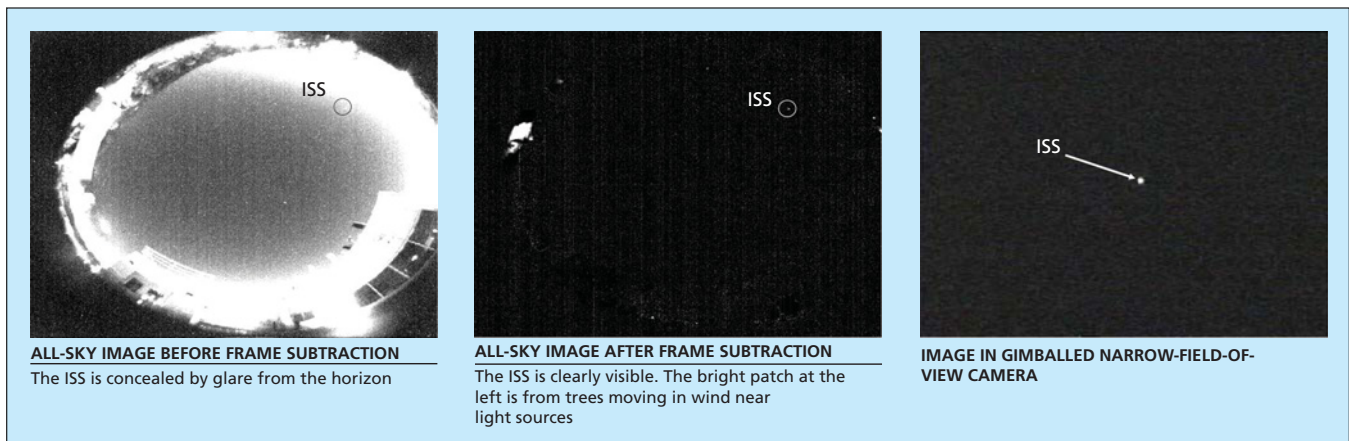


Figure 2. Images of the International Space Station (ISS) were acquired by the prototype apparatus and used to track the ISS as it moved across the sky.

manifests itself in the processed image as a bright spot on a dark background (see Figure 2). The moving target is detected computationally as a spot of pixels brighter than a set threshold level. The location of the target is determined, to within a fraction of a pixel, as a brightness-weighted average pixel location. By use of a straightforward transformation that utilizes the image-detector-plane cal-

ibration, the target location is converted to azimuth and elevation coordinates, then by use of another calibrated transformation, the azimuth and elevation coordinates are converted to gimbal commands for initial aiming of the narrow-field-of-view camera.

Once the narrow-field-of view camera has been initially aimed and has acquired an image of the target, the apparatus

switches into a tracking mode. In this mode, the gimbal commands are formulated to move the image of the target toward the center of the CCD image plane.

*This work was done by Abhijit Biswas, Christopher Assad, Joseph M Kovalik, Be-dabrata Pain, Chris J. Wrigley, and Peter Twiss of Caltech for NASA's Jet Propulsion Laboratory. Further information is contained in a TSP (see page 1). NPO-45237*

## Visual Data Analysis for Satellites

*Stennis Space Center, Mississippi*

The Visual Data Analysis Package is a collection of programs and scripts that facilitate visual analysis of data available from NASA and NOAA satellites, as well as dropsonde, buoy, and conventional *in-situ* observations. The package features utilities for data extraction, data quality control, statistical analysis, and data visualization.

The Hierarchical Data Format (HDF) satellite data extraction routines from NASA's Jet Propulsion Laboratory were customized for specific spatial coverage and file input/output. Statistical analysis

includes the calculation of the relative error, the absolute error, and the root mean square error. Other capabilities include curve fitting through the data points to fill in missing data points between satellite passes or where clouds obscure satellite data. For data visualization, the software provides customizable Generic Mapping Tool (GMT) scripts to generate difference maps, scatter plots, line plots, vector plots, histograms, time-series, and color fill images.

*This program was written by Yee Lau, Sachin Bhate, and Patrick Fitzpatrick of the*

*GeoResources Institute at Mississippi State University for Stennis Space Center.*

*Inquiries concerning rights for its commercial use should be addressed to:*

*Mississippi State University  
P.O. Box 6156*

*Mississippi State, MS 39762-5368*

*Phone No: (228) 688-1157*

*E-mail: fitz@gri.msstate.edu*

*Refer to SSC-00266-1, volume and number of this NASA Tech Briefs issue, and the page number.*

## A Data Type for Efficient Representation of Other Data Types

**Some obstacles to programming of parallel computers are removed.**

*NASA's Jet Propulsion Laboratory, Pasadena, California*

A self-organizing, monomorphic data type denoted a sequence has been conceived to address certain concerns (summarized below) that arise in programming parallel computers. ["Sequence" as used here should not be confused with "sequence" as the word is commonly un-

derstood or with "sequence" as used elsewhere to denote another, polymorphic data type that is also relevant to computer programming.] A sequence in the present sense can be regarded abstractly as a vector, set, bag, queue, or other construct. A sequence is defined in terms of

the behavior of the operators that can be applied to it without any foreknowledge of the underpinnings of its representation or particular implementation.

Heretofore, in programming a parallel computer, it has been necessary for the programmer to state explicitly, at the

outset, what parts of the program and the underlying data structures must be represented in parallel form. Not only is this requirement not optimal from the perspective of implementation; it entails an additional requirement that the programmer have intimate understanding of the underlying parallel structure. Often, it is not possible to have such understanding because hardware and software are designed simultaneously. The present sequence data type overcomes both the implementation and parallel-structure obstacles. In so doing, the sequence data type provides unified means by which the programmer can represent a data structure for natural and automatic decomposition to a parallel computing architecture.

Sequences exhibit the behavioral and structural characteristics of vectors, but the underlying representations are automatically synthesized from combinations of programmers' advice and execution use metrics. Sequences can vary bidirectionally between sparseness and density, making them excellent choices for many

kinds of algorithms. The novelty and benefit of this behavior lies in the fact that it can relieve programmers of the details of implementations.

The creation of a sequence enables decoupling of a conceptual representation from an implementation. In essence, a sequence is a fundamental extension of a vector. In the most general case, the length and internal structure of a sequence can be changed during run time, enabling the efficient addition and removal of elements around given positions. Because sequences are not subject to predefined limits in length, they can be used equally to store small and large collections of elements.

Sequences have efficient representations in both time and space for given patterns of use. When the use pattern of a sequence is simple, then the user has the option of causing its basic operations to be coded in line for maximal efficiency.

The underlying representation of a sequence is a hybrid of representations composed of vectors, linked lists, connected blocks, and hash tables. The inter-

nal structure of a sequence can automatically change from time to time on the basis of how it is being used. Those portions of a sequence where elements have not been added or removed can be as efficient as vectors. As elements are inserted and removed in a given portion, then different methods are utilized to provide both an access and memory strategy that is optimized for that portion and the use to which it is put.

*This work was done by Mark James of Caltech for NASA's Jet Propulsion Laboratory.*

*In accordance with Public Law 96-517, the contractor has elected to retain title to this invention. Inquiries concerning rights for its commercial use should be addressed to:*

*Innovative Technology Assets Management  
JPL*

*Mail Stop 202-233  
4800 Oak Grove Drive  
Pasadena, CA 91109-8099  
(818) 354-2240*

*E-mail: iaoffice@jpl.nasa.gov*

*Refer to NPO-41090, volume and number of this NASA Tech Briefs issue, and the page number.*

## Hand-Held Ultrasonic Instrument for Reading Matrix Symbols

All necessary functions would be performed within a compact package.

*Marshall Space Flight Center, Alabama*

A hand-held instrument that would include an ultrasonic camera has been proposed as an efficient means of reading matrix symbols. The proposed instrument could be operated without mechanical raster scanning. All electronic functions from excitation of ultrasonic pulses through final digital processing for decoding matrix symbols would be performed by dedicated circuitry within the single, compact instrument housing.

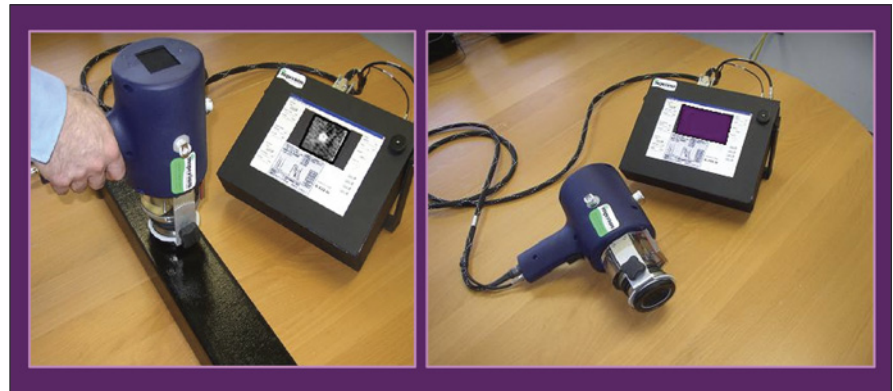
The instrument (see figure) would be placed on a selected area on an object of interest believed or suspected to contain a matrix symbol (hereafter denoted, simply, the target). Intimate contact for the purpose of coupling of low-energy ultrasound would be ensured by use of either a flexible membrane camera face or a replaceable gel pad. Ultrasound pulses would be transmitted from a transducer, through the membrane or gel pad, into the target. A portion of each ultrasonic pulse, as modified by any matrix symbol present in the target, would be reflected through the membrane or gel pad to

an ultrasound-imaging integrated-circuit chip, which would convert the resulting spatial variation of ultrasound pressure to voltages that could be used to construct a video image of the matrix symbol (if any).

A set of circuit boards above the ultrasound-imaging chip converts the output of the chip into a useful video format and would coordinate timing between the transducer pulses and the acquisition and processing of image data. The

system is fully portable and battery powered. The instrument includes the following other boards:

- A pulser board would control the current pulses that drive the acoustic transducer.
- A board comprising a liquid-crystal display unit and its driver circuitry would enable display of the video image in the future. It could include a decoder board that would translate the video image of a matrix symbol into a recog-



An Ultrasonic Camera and associated electronic circuitry would generate and decode a video image of a matrix symbol hidden below the surface of the target.

nizable set of binary data. This board would be identical to that used in a commercial bar-code reader. Upon observing a matrix symbol in the video display, the operator would press a trigger switch to activate the decoder. The

output of the decoder could be made available to a data-collection system for recording of the information in the matrix symbol.

*This work was done by Harry F. Schramm of Marshall Space Flight Center; Robert S.*

*Lasser and John P. Kula of Imperium, Inc.; and John W. Gurney and Ephraim D. Lior formerly of Imperium, Inc. For more information, contact Sammy Nabors, MSFC Commercialization Assistance Lead, at sammy.a.nabors@nasa.gov. MFS-31782-1*





## Broadband Microstrip-to-Coplanar Strip Double-Y Balun

This balun is compact, broadband, and can be fabricated easily.

NASA's Jet Propulsion Laboratory, Pasadena, California

A new version of the double-Y balun, transitioning from an unbalanced microstrip to a balanced coplanar strip (CPS) line, has been designed to feed a complementary spiral antenna with an input impedance of  $100\ \Omega$ . Various ver-

sions of the double-Y balun have been investigated in previous literature for use with balanced mixers and pulsed antennas. Of the previous versions, the double-Y balun transitioning from a coplanar waveguide (CPW) to CPS was

found to exhibit the widest bandwidth of operation while having little metal content (attractive for use in ground-penetrating radar applications). However, the double-Y balun transitioning from a CPW to CPS requires coplanar wave-

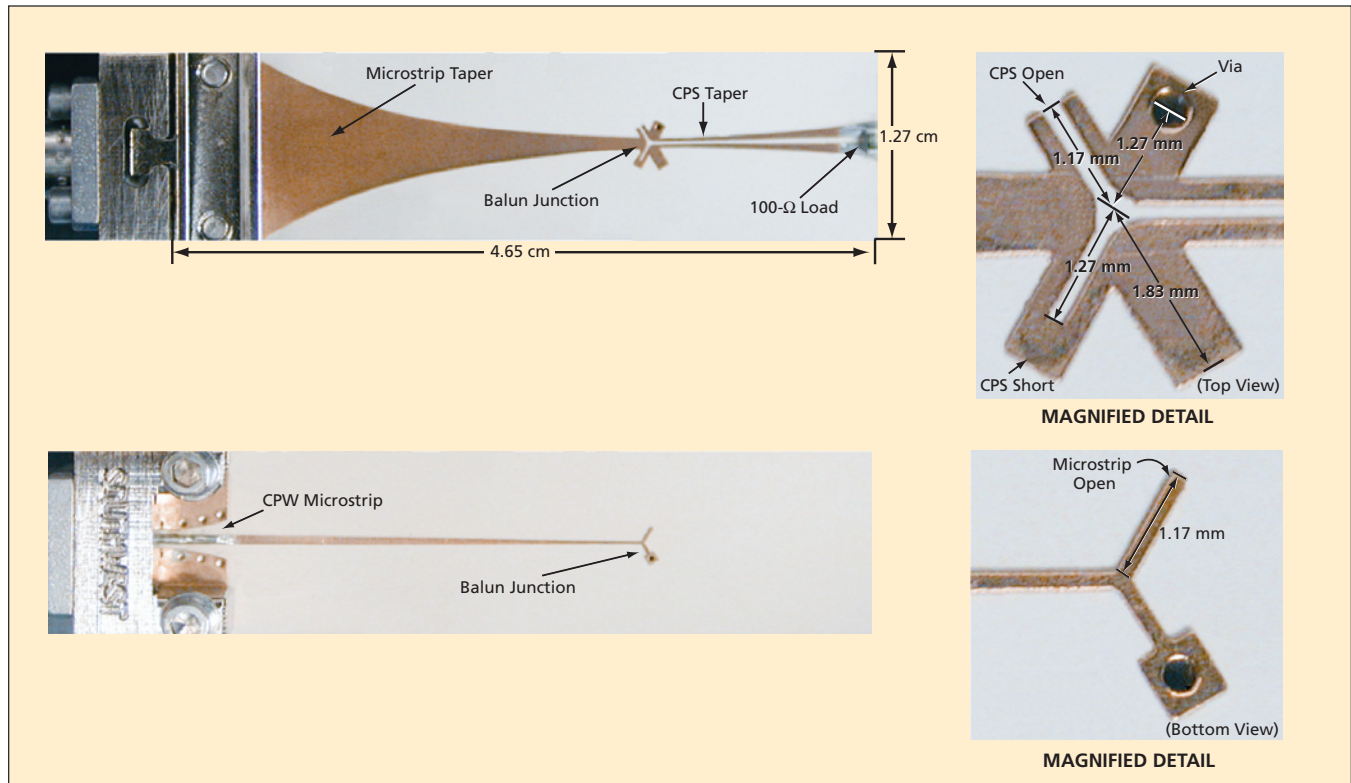


Figure 1. The New Double-Y Balun, shown here in top and bottom views, is designed to feed a  $100\text{-}\Omega$  complementary spiral antenna (balun is manufactured on  $0.635\text{-mm}$  thick substrate). The panels on the right are expanded views showing greater detail.

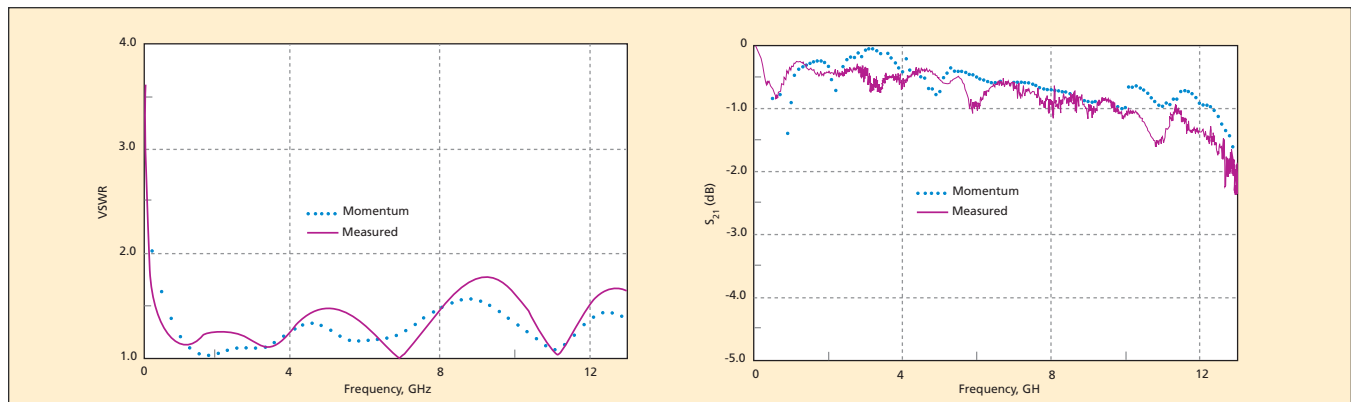


Figure 2 Preliminary VSWR and Insertion Loss Data: (a) Plot of measured vs. computed VSWR is shown for the double-Y balun in Figure 1 terminated with a  $100\text{-}\Omega$  load resistor and (b) a plot of measured vs. computed insertion loss is shown for the balun in back-to-back configuration.

guide bridges at the junction; the inductive behavior of the bridges, in addition to CPW parasitic resonances, degrades the passband performance of the balun.

The new double-Y balun transitions from a microstrip line with truncated ground plane to a CPS line. The balun does not employ CPW lines; hence, CPW bridges are not required at the junction. In addition, the balun does not exhibit CPW parasitic resonances, thereby improving passband performance.

Figure 1 illustrates the new version of the double-Y balun designed to feed a complementary spiral antenna. Panels on the right illustrate an expanded view of the balun junction. Preliminary voltage standing-wave ratio (VSWR) and insertion loss data are illustrated in Figure 2. Measured data were compared with numerical results computed using Momentum. It is seen that the balun exhibits a VSWR of less than 1.5 from 400 MHz to 8 GHz and a VSWR of less than 1.8 up to 13 GHz. The

VSWR can be reduced further by reducing reflections from the balun junction and load resistor. Also, the balun is seen to exhibit an insertion loss of less than 1.5 dB up to 12 GHz. Further work involves characterizing the balun's performance when feeding a complementary spiral antenna.

*This work was done by Jaikrishna Venkatesan of Caltech for NASA's Jet Propulsion Laboratory. Further information is contained in a TSP (see page 1). NPO-42763*

---

## A Topographical Lidar System for Terrain-Relative Navigation

**Demand for memory is reduced by digitizing over a limited altitude range.**

*NASA's Jet Propulsion Laboratory, Pasadena, California*

An imaging lidar system is being developed for use in navigation, relative to the local terrain. This technology will potentially be used for future spacecraft landing on the Moon. Systems like this one could also be used on Earth for diverse purposes, including mapping terrain, navigating aircraft with respect to terrain and military applications. The system has been field-tested aboard a helicopter in the Mojave Desert.

The use of imaging lidar systems to generate digital data sets equivalent to topographical maps is well established. Such systems are commercially available and often denoted simply as topographical or topographic lidar systems. As in other imaging lidar systems, a gimballed, actuated mirror is used to raster-scan a narrow laser beam across a field of view, the laser beam is emitted in short laser pulses, the pulses are reflected from the terrain, and the distance to the terrain in a given direction is determined from the total time of flight from the emission of the outgoing pulse to the receipt of the

reflected pulse. Then the combination of direction (azimuth and elevation angles associated with the mirror orientation) and the range (distance) for each such direction constitute raw data that can be used to generate a topographical map of the terrain.

When this system was designed, digitizers with sufficient sampling rate (2 GHz) were only available with very limited memory. Also, it was desirable to limit the amount of data to be transferred between the digitizer and the mass storage between individual frames. One of the novelty design features of this system was to design the system around the limited amount of memory of the digitizer. The system is required to operate over an altitude (distance) range from a few meters to  $\approx 1$  km, but for each scan across the full field of view, the digitizer memory is only able to hold data for an altitude range no more than 100 m. Therefore, the acquisition of data is limited to an altitude range 100 m wide in the following way: Initially a pulse is emitted and digitized over an altitude

range of 5 km. This process is repeated four more times, and the median time of the first return pulse of all five measurements is computed as the distance from which to expect future laser pulse to be reflected. A distance of 50 m is subtracted from the expected distance and the resulting distance is fed as a programming input to a programmable-delay pulse generator, which is triggered by the outgoing laser pulse and which, in turn, turns on the digitizer after the programmed delay. Thus, the digitizer is started at 50 m before the expected receipt of the return pulse. The digitizer then operates over an altitude interval of 100 m; it is stopped at 50 m after the expected return of the receipt of the return pulse.

*This work was done by Carl Christian Liebe, Gary Spiers, Randy Bartman, Raymond Lam, James Alexander, James Montgomery, Hannah Goldberg, Andrew Johnson, Patrick Meras, and Peter Palacios of Caltech for NASA's Jet Propulsion Laboratory. Further information is contained in a TSP (see page 1). NPO-44586*

---

## Programmable Low-Voltage Circuit Breaker and Tester

**This system could also detect some faults before turning on power.**

*John F. Kennedy Space Center, Florida*

An instrumentation system that would comprise a remotely controllable and programmable low-voltage circuit breaker plus several electric-circuit-testing subsystems has been conceived, originally for use aboard a spacecraft during all phases of operation from pre-launch testing through launch, ascent, orbit, de-

scend, and landing. The system could also be adapted to similar use aboard aircraft. In comparison with remotely controllable circuit breakers heretofore commercially available, this system would be smaller, less massive, and capable of performing more functions, as needed for aerospace applications.

The circuit breaker in this system could be set open or closed and could be monitored, all remotely. Trip current could be set at a specified value or could be made to follow a trip curve (a specified trip current as a function of time). In a typical application, there might be a requirement to set a lower trip current

or lower trip-curve values to protect circuits during initial testing, and to set a default higher trip current during subsequent pre-launch and launch operations.

In the open state of the circuit breaker, one of the circuit-testing subsystems could obtain electrical-resistance readings on the load side as indications of whether faults are present, prior to switching the circuit breaker closed. Should a fault be detected, another circuit-testing subsystem could perform time-domain reflectometry, which would be helpful in locating the fault. On the power-line side, still another circuit-testing subsystem could take a voltage reading, as an indication

of whether the proper voltage is present, prior to switching the circuit breaker closed.

The system would be contained in a housing, with input, output, and data/control connectors on the rear surface. All monitoring, control, and programming functions would ordinarily be performed from a remote console. On the front surface, there would be a push-button switch for optionally locally setting the circuit breaker in the open or closed state, plus a lamp that would provide a local visual indication of whether the circuit breaker was in the open (initially set), closed, or open (tripped) state.

The aforementioned monitoring, testing, state-setting, and trip-current-setting functions would be effected by circuitry on an integrated-circuit card inside the housing. Also on the card would be (1) input and output circuitry for remote monitoring and control and (2) a tag random-access memory as an electronic means of identifying the system by serial number, location, a reference designation, and operational characteristics.

*This work was done by Terry Greenfield of ASRC Aerospace Corp. for Kennedy Space Center. For further information, contact the Kennedy Innovative Partnerships Program Office at (321) 861-7158. KSC-12742*

## Electronic Switch Arrays for Managing Microbattery Arrays

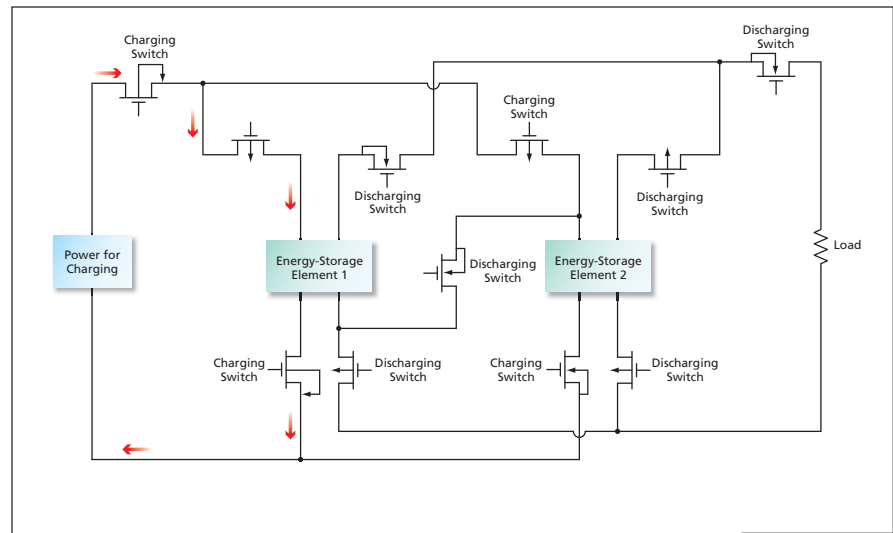
Array circuitry is dynamically configured to optimize performance and disconnect defective elements.

NASA's Jet Propulsion Laboratory, Pasadena, California

Integrated circuits have been invented for managing the charging and discharging of such advanced miniature energy-storage devices as planar arrays of microscopic energy-storage elements [typically, microscopic electrochemical cells (microbatteries) or microcapacitors]. The architecture of these circuits enables implementation of the following energy-management options:

- Dynamic configuration of the elements of an array into a series or parallel combination of banks (subarrays), each array comprising a series or parallel combination of elements;
- Direct addressing of individual banks for charging and/or discharging; and
- Disconnection of defective elements and corresponding reconfiguration of the rest of the array to utilize the remaining functional elements to obtain the desired voltage and current performance.

One of the reasons for fabricating microbattery and microcapacitor arrays is that the array form affords partial immunity to defects in individual energy-storage elements. Defective energy-storage elements act as loads on the functional ones, thereby reducing the capacity of an overall array. By enabling the disconnection of defective elements and reconfiguration of the rest of the array, the present invention offers practical means to realize this partial immunity. In addition, the invention provides for interrogating individual cells and banks in the



**Two Energy-Storage Elements** can be connected, individually or together in series or parallel, to the power source or the load by closing or opening the appropriate subset of switching transistors. This example has been greatly oversimplified for the sake of illustrating the basic principle; a typical practical circuit would contain many more energy-storage elements and switches.

array and charging them at the current-vs.-time or voltage-vs.-time characteristics needed for maximizing the life of the array.

An integrated circuit according to the invention consists partly of a planar array of field-effect transistors that function as switches for routing electric power among the energy-storage elements, the power source, and the load (see figure). To connect the energy-storage elements to the power source for charging, a specific subset of switches is closed; to connect the energy-storage el-

ements to the load for discharging, a different specific set of switches is closed.

Also included in the integrated circuit, but omitted from the figure for the sake of simplicity, is circuitry for monitoring and controlling charging and discharging. The control and monitoring circuitry, the switching transistors, and interconnecting metal lines are laid out on the integrated-circuit chip in a pattern that registers with the array of energy-storage elements. There is a design option to either (1) fabricate the energy-storage elements in the cor-

responding locations on, and as an integral part of, this integrated circuit; or (2) following a flip-chip approach, fabricate the array of energy-storage elements on a separate integrated-circuit chip and then align and bond the two chips together.

*This work was done by Mohammad Mojaradi, Mahmoud Alahmad, Vinesh Sukumar,*

*Fadi Zghoul, Kevin Buck, Herbert Hess, Harry Li, and David Cox of Caltech for NASA's Jet Propulsion Laboratory. Further information is contained in a TSP (see page 1).*

*In accordance with Public Law 96-517, the contractor has elected to retain title to this invention. Inquiries concerning rights for its commercial use should be addressed to:*

*Innovative Technology Assets Management*

*JPL*

*Mail Stop 202-233*

*4800 Oak Grove Drive*

*Pasadena, CA 91109-8099*

*(818) 354-2240*

*E-mail: iaoffice@jpl.nasa.gov*

*Refer to NPO-43318, volume and number of this NASA Tech Briefs issue, and the page number.*

## Lower-Dark-Current, Higher-Blue-Response CMOS Imagers

Semiconductor junctions are relocated away from Si/SiO<sub>2</sub> interfaces.

NASA's Jet Propulsion Laboratory, Pasadena, California

Several improved designs for complementary metal oxide/semiconductor (CMOS) integrated-circuit image detectors have been developed, primarily to reduce dark currents (leakage currents) and secondarily to increase responses to blue light and increase signal-handling capacities, relative to those of prior CMOS imagers. The main conclusion that can be drawn from a study of the causes of dark currents in prior CMOS imagers is that dark currents could be reduced by relocating p/n junctions away from Si/SiO<sub>2</sub> interfaces. In addition to reflecting this conclusion, the improved designs include several other features to counteract dark-current mechanisms and enhance performance.

The left half of the figure illustrates two of the improved designs, in which p-

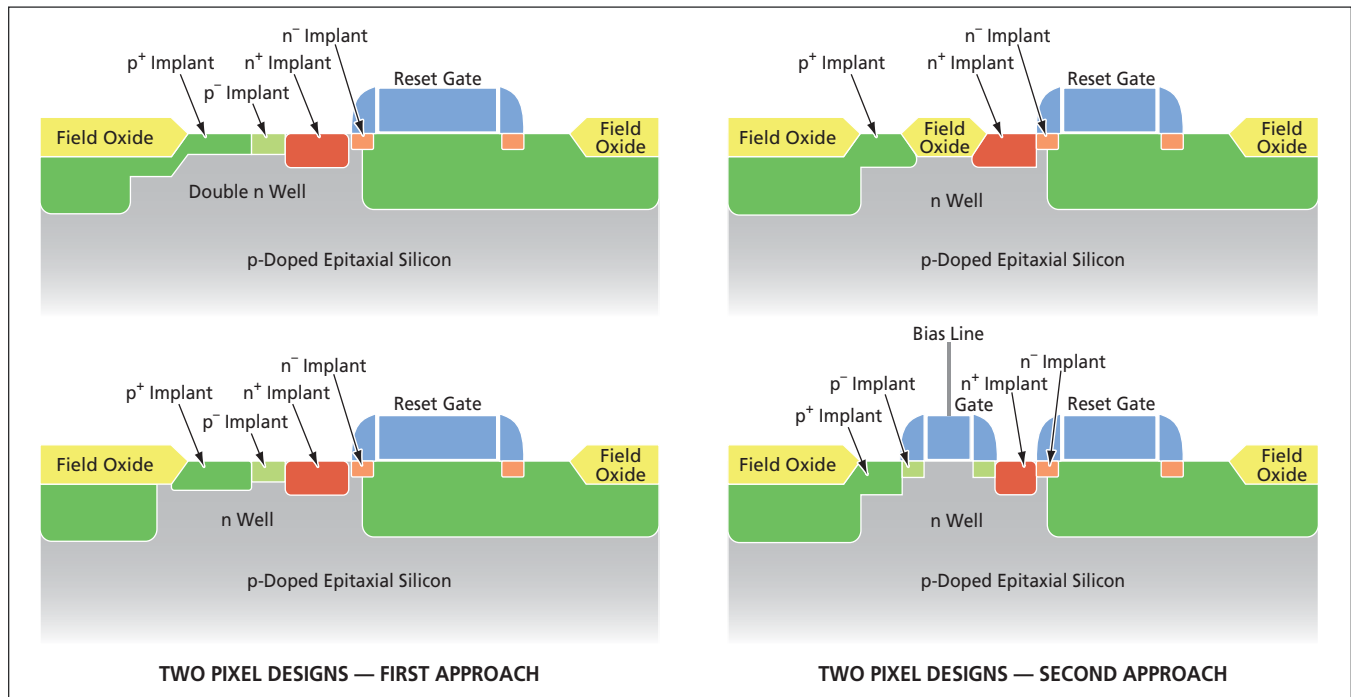
doped implants are added, variously, underneath and/or at the edges of the field oxide regions. These implants hold the Si/SiO<sub>2</sub> interfaces in thermal equilibrium and prevent generation of dark current at the interfaces. In covering the field oxide, the p implants separate the p/n junctions from the Si/SiO<sub>2</sub> interfaces, so that the interfacial component of the dark current (which is the major component) is greatly reduced.

Beyond a certain electric strength, the leakage current depends very strongly on the strength of the electric field. In order to reduce electric fields in the reverse-biased junctions, the p wells are separated from the n wells. A double n well in each pixel is preferred, both for increased photocarrier-collection efficiency and for tailoring the

doping so that the electric field in the transition region between p<sup>+</sup>-to-n-well region is low.

For electrical connections to the photodiodes, which also act as the sources of reset field-effect transistors, n<sup>+</sup> implants are necessary. Unfortunately, the p<sup>+</sup>/n<sup>+</sup> junctions heretofore associated with such implants are undesirable because they contain high electric fields, which give rise to significant tunneling currents, which, in turn, are components of dark currents. In these designs, p-implants are added at the surfaces to tailor the doping from p<sup>+</sup> accumulation layers to n<sup>+</sup> source layers, thereby reducing tunneling currents.

Two of the improved designs illustrated in the right half of the figure follow an alternative approach to tailoring



These Cross Sections of a Pixel in a CMOS imager represent four designs that provide for reduction of dark currents in different ways.



appropriate transitions between surface  $p^+$  accumulation layers and  $n^+$  source layers. In this approach, field oxide regions or gates are positioned to separate the  $p^+$  and  $n^+$  regions. A gate separating the  $p$  and  $n$  regions can be DC-biased to prevent conduction of current underneath the gate, thereby providing sufficient isolation between the  $p$  and the  $n$  regions. Alternatively, instead of being DC-biased, the  $p/n$ -separating gate in each pixel can be electrically tied to the reset gate of that pixel to obtain a more-compact layout.

According to each of these designs, a double  $p/n$  junction is formed in each pixel: one junction near the surface be-

tween the  $p^+$  and the  $n$  well, the other in the bulk between the  $n$  well and the  $p$ -doped epitaxial silicon. The near-surface junction provides increased response to blue light because blue photons are absorbed close to the surface. In addition, the double junction increases the pixel capacitance, thereby imparting larger signal-handling capacity to a pixel. This increase in capacitance is particularly beneficial in an imager having small pixels, wherein the limited size of photodiodes causes pixel capacitance to be extremely small.

*This work was done by Bedabrata Pain, Thomas Cunningham, and Bruce Hancock*

*of Caltech for NASA's Jet Propulsion Laboratory.*

*In accordance with Public Law 96-517, the contractor has elected to retain title to this invention. Inquiries concerning rights for its commercial use should be addressed to:*

*Innovative Technology Assets Management  
JPL*

*Mail Stop 202-233  
4800 Oak Grove Drive  
Pasadena, CA 91109-8099  
(818) 354-2240*

*E-mail: [iaoffice@jpl.nasa.gov](mailto:iaoffice@jpl.nasa.gov)*

*Refer to NPO-41224, volume and number of this NASA Tech Briefs issue, and the page number.*





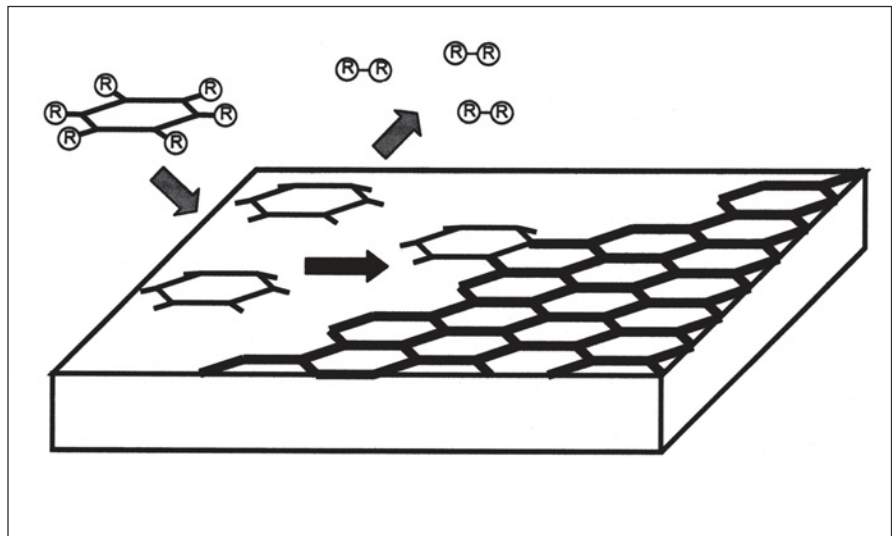
## Fabricating Large-Area Sheets of Single-Layer Graphene by CVD

Such sheets are components for high-speed digital and RF electronics for defense and commercial communications.

NASA's Jet Propulsion Laboratory, Pasadena, California

This innovation consists of a set of methodologies for preparing large area ( $>1 \text{ cm}^2$ ) domains of single-atomic-layer graphite, also called graphene, in single (two-dimensional) crystal form. To fabricate a single graphene layer using chemical vapor deposition (CVD), the process begins with an atomically flat surface of an appropriate substrate and an appropriate precursor molecule containing carbon atoms attached to substituent atoms or groups. These molecules will be brought into contact with the substrate surface by being flowed over, or sprayed onto, the substrate, under CVD conditions of low pressure and elevated temperature. Upon contact with the surface, the precursor molecules will decompose. The substituent groups detach from the carbon atoms and form gas-phase species, leaving the unfunctionalized carbon atoms attached to the substrate surface. These carbon atoms will diffuse upon this surface and encounter and bond to other carbon atoms. If conditions are chosen carefully, the surface carbon atoms will arrange to form the lowest energy single-layer structure available, which is the graphene lattice that is sought.

A precursor may contain only one carbon atom, such as methane or derivatized methane (e.g., carbon tetrachloride). However, it is more likely that the best precursor molecule will be an aromatic compound that has at least 6 carbon atoms already arranged in the aromatic structure of hexagonal rings, because this will be the geometry of the carbon atoms in the final graphene material. An example of a possible candidate precursor molecule is hexachlorobenzene, an aromatic molecule containing six carbon atoms in a ring, each of which is bound to one additional chlorine atom. In this molecule, the carbon-chlorine bonds are weak enough that they will break under reasonable CVD conditions (a few hundred degrees C); the chlorine atoms will form  $\text{Cl}_2$  molecules that will escape into the gas phase, while the six-membered carbon



**Growth of a Graphene Sheet by CVD** using an aromatic molecular precursor gas, shown here as a six-membered ring of carbon atoms, each of which is attached to one additional  $\text{-R}$  substituent. Carbon-containing precursor molecules impinge upon a substrate and decompose, resulting in gaseous  $\text{R}_2$  products and surface-bound rings of carbon atoms. These six-membered rings can maintain their structure as they diffuse toward, and bind to, the growing edge of the hexagonal carbon graphene lattice as shown.

ring will be released upon the substrate surface. If conditions are not too extreme, this six-membered ring will be able to diffuse across the substrate surface while maintaining its structural integrity, eventually encountering other rings of carbon atoms from other precursor molecules. These multiple carbon rings will bond together, their constituent carbon atoms binding together to form the lowest energy structure available — the graphene lattice.

Another method for creating the graphene lattice includes metal-catalyzed CVD, in which the decomposition of the precursor molecules is initiated by the catalytic action of a catalytic metal upon the substrate surface. Another type of metal-catalyzed CVD has the entire substrate composed of catalytic metal, or other material, either as a bulk crystal or as a thin layer of catalyst deposited upon another surface. In this case, the precursor molecules decompose directly upon contact with the substrate, releasing their atoms and forming the graphene sheet.

Atomic layer deposition (ALD) can also be used. In this method, a substrate surface at low temperature is covered with exactly one monolayer of precursor molecules (which may be of more than one type). This is heated up so that the precursor molecules decompose and form one monolayer of the target material.

*This work was done by Michael Bronikowski and Harish Manohara of Caltech for NASA's Jet Propulsion Laboratory. Further information is contained in a TSP (see page 1).*

*In accordance with Public Law 96-517, the contractor has elected to retain title to this invention. Inquiries concerning rights for its commercial use should be addressed to:*

*Innovative Technology Assets Management  
JPL*

*Mail Stop 202-233  
4800 Oak Grove Drive  
Pasadena, CA 91109-8099*

*E-mail: iaoffice@jpl.nasa.gov*

*Refer to NPO-45298, volume and number of this NASA Tech Briefs issue, and the page number.*





## Support for Diagnosis of Custom Computer Hardware

The Coldfire SDN Diagnostics software is a flexible means of exercising, testing, and debugging custom computer hardware. The software is a set of routines that, collectively, serve as a common software interface through which one can gain access to various parts of the hardware under test and/or cause the hardware to perform various functions. The routines can be used to construct tests to exercise, and verify the operation of, various processors and hardware interfaces. More specifically, the software can be used to gain access to memory, to execute timer delays, to configure interrupts, and configure processor cache, floating-point, and direct-memory-access units.

The software is designed to be used on diverse NASA projects, and can be customized for use with different processors and interfaces. The routines are supported, regardless of the architecture of a processor that one seeks to diagnose. The present version of the software is configured for Coldfire processors on the Subsystem Data Node processor boards of the Solar Dynamics Observatory. There is also support for the software with respect to Mongoose V, RAD750, and PPC405 processors or their equivalents.

*This program was written by Dwaine S. Molock of Goddard Space Flight Center. For further information, contact the Goddard Innovative Partnerships Office at (301) 286-5810. GSC-15478-1*

## Providing Goal-Based Autonomy for Commanding a Spacecraft

A computer program for use aboard a scientific-exploration spacecraft autonomously selects among goals specified in high-level requests and generates corresponding sequences of low-level commands, understandable by spacecraft systems. (As used here, “goals” signifies specific scientific observations.) From a dynamic, onboard set of goals that could oversubscribe spacecraft resources, the program selects a non-oversubscribing subset that maximizes a

quality metric. In an early version of the program, the requested goals are assumed to have fixed starting times and durations. Goals can conflict by exceeding a limit on either the number of separate goals or the number of overlapping goals making demands on the same resource.

The quality metric used in this version is chosen to ensure that a goal will never be replaced by another having lower priority. At any time, goals can be added or removed, or their priorities can be changed, and the “best” goal will be selected. Once a goal has been selected, the program implements a robust, flexible approach to generation of low-level commands: Rather than generate rigid sequences with fixed starting times, the program specifies flexible sequences that can be altered to accommodate run time variations.

*This program was written by Gregg Rabideau, Steve Chien, and Ning Liu of Caltech for NASA’s Jet Propulsion Laboratory. Further information is contained in a TSP (see page 1).*

*This software is available for commercial licensing. Please contact Karina Edmonds of the California Institute of Technology at (626) 395-2322. Refer to NPO-44541.*

## Dynamic Method for Identifying Collected Sample Mass

G-Sample is designed for sample collection missions to identify the presence and quantity of sample material gathered by spacecraft equipped with end effectors. The software method uses a maximum-likelihood estimator to identify the collected sample’s mass based on onboard force-sensor measurements, thruster firings, and a dynamics model of the spacecraft. This makes sample mass identification a computation rather than a process requiring additional hardware.

Simulation examples of G-Sample are provided for spacecraft model configurations with a sample collection device mounted on the end of an extended boom. In the absence of thrust knowledge errors, the results indicate that G-Sample can identify the amount of collected sample mass to within 10 grams (with 95-percent confidence) by using a force sensor with a noise and quantiza-

tion floor of 50 micrometers. These results hold even in the presence of realistic parametric uncertainty in actual spacecraft inertia, center-of-mass offset, and first flexibility modes.

Thrust profile knowledge is shown to be a dominant sensitivity for G-Sample, entering in a nearly one-to-one relationship with the final mass estimation error. This means thrust profiles should be well characterized with onboard accelerometers prior to sample collection. An overall sample-mass estimation error budget has been developed to approximate the effect of model uncertainty, sensor noise, data rate, and thrust profile error on the expected estimate of collected sample mass.

*This program was written by John Carson of Caltech for NASA’s Jet Propulsion Laboratory. Further information is contained in a TSP (see page 1).*

*This software is available for commercial licensing. Please contact Karina Edmonds of the California Institute of Technology at (626) 395-2322. Refer to NPO-44403.*

## Optimal Planning and Problem-Solving

CTAEMS MDP Optimal Planner is a problem-solving software designed to command a single spacecraft/rover, or a team of spacecraft/rovers, to perform the best action possible at all times according to an abstract model of the spacecraft/rover and its environment. It also may be useful in solving logistical problems encountered in commercial applications such as shipping and manufacturing.

The planner reasons around uncertainty according to specified probabilities of outcomes using a plan hierarchy to avoid exploring certain kinds of sub-optimal actions. Also, planned actions are calculated as the state-action space is expanded, rather than afterward, to reduce by an order of magnitude the processing time and memory used. The software solves planning problems with actions that can execute concurrently, that have uncertain duration and quality, and that have functional dependencies on others that affect quality. These problems are modeled in a hierarchical planning language called C\_TAEMS, a derivative of the TAEMS language for

specifying domains for the DARPA Coordinators program.

In realistic environments, actions often have uncertain outcomes and can have complex relationships with other tasks. The planner approaches problems by considering all possible actions that may be taken from any state reachable from a given, initial state, and from within the constraints of a given task hierarchy that specifies what tasks may be performed by which team member.

*This program was written by Bradley Clement, Steven Schaffer, and Gregg Rabideau of Caltech for NASA's Jet Propulsion Laboratory. Further information is contained in a TSP (see page 1).*

*This software is available for commercial licensing. Please contact Karina Edmonds of the California Institute of Technology at (626) 395-2322. Refer to NPO-44019.*

---

### **Attitude-Control Algorithm for Minimizing Maneuver Execution Errors**

A G-RAC attitude-control algorithm is used to minimize maneuver execution

error in a spacecraft with a flexible appendage when said spacecraft must induce translational momentum by firing (in open loop) large thrusters along a desired direction for a given period of time. The controller is dynamic with two integrators and requires measurement of only the angular position and velocity of the spacecraft. The global stability of the closed-loop system is guaranteed without having access to the states describing the dynamics of the appendage and with severe saturation in the available torque.

Spacecraft apply open-loop thruster firings to induce a desired translational momentum with an extended appendage. This control algorithm will assist this maneuver by stabilizing the attitude dynamics around a desired orientation, and consequently minimize the maneuver execution errors.

*This work was done by Behçet Açikmeşe of Caltech for NASA's Jet Propulsion Laboratory.*

*The software used in this innovation is available for commercial licensing. Please contact Karina Edmonds of the California Institute of Technology at (626) 395-2322. Refer to NPO-44376.*

---

### **Grants Document-Generation System**

The Grants Document-Generation System (GDGS) software allows the generation of official grants documents for distribution to the appropriate parties. The documents are created after the selection and entry of specific data elements and clauses. GDGS is written in Cold Fusion that resides on an SQL2000 database and is housed on-site at Goddard Space Flight Center. It includes access security written around GSFC's (Goddard Space Flight Center's) LIST system, and allows for the entry of Procurement Request information necessary for the generation of the resulting Grant Award.

*This work was done by Terri Hairrell, Lev Kreymer, Greg Martin, and Patrick Sheridan of the INDUS Corporation for Goddard Space Flight Center. For further information, contact the Goddard Innovative Partnerships Office at (301) 286-5810. GSC-15187-1*



## Heat-Storage Modules Containing $\text{LiNO}_3 \cdot 3\text{H}_2\text{O}$ and Graphite Foam

Heat capacity per unit volume has been increased.

NASA's Jet Propulsion Laboratory, Pasadena, California

A heat-storage module based on a commercial open-cell graphite foam (Poco-Foam or equivalent) imbued with lithium nitrate trihydrate ( $\text{LiNO}_3 \cdot 3\text{H}_2\text{O}$ ) has been developed as a prototype of other such modules for use as short-term heat sources or heat sinks in the temperature range of approximately 28 to 30 °C. In this module, the  $\text{LiNO}_3 \cdot 3\text{H}_2\text{O}$  serves as a phase-change heat-storage material and the graphite foam as thermally conductive filler for transferring heat to or from the phase-change material. In comparison with typical prior heat-storage modules in which paraffins are the phase-change materials and aluminum fins are the thermally conductive fillers, this module has more than twice the heat-storage capacity per unit volume.

The use of  $\text{LiNO}_3 \cdot 3\text{H}_2\text{O}$  as a phase-change heat-storage material is not new in itself, but heretofore, it has been used with aluminum fins. Open-cell graphite foam has been used as the thermally conductive filler material in conjunction with paraffin phase-change materials in some prior heat-storage modules but, heretofore, it has not been used with  $\text{LiNO}_3 \cdot 3\text{H}_2\text{O}$  because graphite foam is hydrophobic and, therefore not readily wet by  $\text{LiNO}_3 \cdot 3\text{H}_2\text{O}$ . The novelty of the present development lies in the choice of materials to make it possible to use graphite foam as the filler with



The **Components Shown Separately** here were assembled to make a heat-storage module. Prior to sealing the module, the open-cell graphite foam was filled with molten  $\text{LiNO}_3 \cdot 3\text{H}_2\text{O}$  containing small proportions of a surfactant and a freezing catalyst.

$\text{LiNO}_3 \cdot 3\text{H}_2\text{O}$  in order to exploit the greater (relative to aluminum) specific thermal conductivity of graphite to reduce the mass of filler needed to obtain a given level of thermal performance.

The prototype heat-storage module consists of an  $\text{LiNO}_3 \cdot 3\text{H}_2\text{O}$ -imbued open-cell graphite foam core of 76-percent porosity in an aluminum housing that has a ribbed top that provides a rigid mounting surface for electronics. During fabrication, grooves to receive the ribs were cut into the open-cell graphite foam core (see figure). To overcome the hydrophobicity of the graphite foam to enable the core to absorb the  $\text{LiNO}_3 \cdot 3\text{H}_2\text{O}$ , an organosilicon surfactant was added to the molten

$\text{LiNO}_3 \cdot 3\text{H}_2\text{O}$  in the proportion of 0.3 mass percent.

Also added to the  $\text{LiNO}_3 \cdot 3\text{H}_2\text{O}$  was 1 mass percent of zinc nitrate, which serves as a freezing catalyst to reduce, to an interval of 2 °C, what would otherwise be the susceptibility of  $\text{LiNO}_3 \cdot 3\text{H}_2\text{O}$  to freezing supercooling by as much as 35 °C. With this catalyst, the  $\text{LiNO}_3 \cdot 3\text{H}_2\text{O}$  freezes at 28 °C when cooled from a higher temperature and melts at 30 °C when warmed from a lower temperature.

*This work was done by Michael Pauken and Nickolas Emis of Caltech and John Boole of XC Associates for NASA's Jet Propulsion Laboratory. For more information, contact [iaoffice@jpl.nasa.gov](mailto:iaoffice@jpl.nasa.gov). NPO-44169*

## Precipitation-Strengthened, High-Temperature, High-Force Shape Memory Alloys

Shape memory alloys capable of performing up to 400 °C have been developed for use in solid-state actuator systems.

John H. Glenn Research Center, Cleveland, Ohio

Shape memory alloys (SMAs) are an enabling component in the development of compact, lightweight, durable, high-force actuation systems particularly

for use where hydraulics or electrical motors are not practical. However, commercial shape memory alloys based on NiTi are only suitable for applications

near room temperature, due to their relatively low transformation temperatures, while many potential applications require higher temperature capability.

Consequently, a family of  $(\text{Ni,Pt})_{1-x}\text{Ti}_x$  shape memory alloys with Ti concentrations  $x \leq 50$  atomic percent and Pt contents ranging from about 15 to 25 at.% have been developed for applications in which there are requirements for SMA actuators to exert high forces at operating temperatures higher than those of conventional binary NiTi SMAs. These alloys can be heat treated in the range of 500 °C to produce a series of fine precipitate phases that increase the strength of alloy while maintaining a high transformation temperature, even in Ti-lean compositions.

The absolute minimum requirement for determining the operating temperature of an SMA is the temperature of the martensite-to-austenite, solid-state phase transformation, which is the source of the shape memory behavior. However, the present high-temperature, high-force SMAs can be used at temperatures up to 400 °C not only because they exhibit a range of high transformation temperatures, but because these materials also exhibit high strength (resistance to dislocation mediated deformation processes) in both the austenite and martensite phases, have a relatively high recovery temperature, and also exhibit excellent dimensional stability (little or no irrecoverable strain component during the transformation process). Consequently, these alloys are attractive for use in performing actuator and control functions particularly in the aggressive environments often encountered in aerospace, automotive, and down-hole energy exploration applications.

The composition of an alloy of this type is given generally by the empirical formula  $\text{Ni}_{x-y-z}\text{Pt}_y\text{M}_z\text{Ti}_{100-x}$  where M can be Au, Pd, or Cu;  $x$ ,  $y$ , and  $z$  are atomic percentages;  $50 \leq x \leq 55$ ;  $10 \leq y \leq 30$ ;  $0 \leq z \leq 10$ . These alloys are precipitation-hardenable, but unlike in prior Ti-rich NiTi alloys, the slightly Ti-lean composition prevents the formation of the  $\text{Ti}_2\text{Ni}$  phase, which is a coarse globular phase that cannot be thermally tailored in as much as it appears during solidification. Instead, one can rely on precipitation of fine  $(\text{Ni,Pt})_3\text{Ti}_2$  structures and other intermetallic phases for enhanced performance. These precipitates are often lath-like in structure and, in many cases, submicron in size. The precipitate volume fraction can also be tailored through heat treatment and alloy composition. These precipitates result in additional strengthening of the austenite (high-temperature) matrix phase and increase the resistance of the martensite phase against slip, without exerting a significant effect on the detwinning stress. Thus, the overall effects are greater specific work output with better dimensional stability, and superior mechanical properties, especially at high temperatures.

The desirable properties of these alloys include the following:

- Their transformation temperatures variously remain stable or increase with aging time.
- They exhibit specific-work-output levels  $>9 \text{ J/cm}^3$  and good work performance, comparable to those of conventional binary NiTi alloys.
- Unlike NiTi and other NiTi-based ter-

nary SMAs, these alloys do not exhibit transformation temperatures lower than those of corresponding stoichiometric alloys; indeed, these alloys exhibit transformation temperatures higher than those of similar alloys that have Ti-rich compositions.

- Unlike in the prior NiTi-based ternary SMA alloys, which exhibit decreases in transformation temperatures with increased aging time or thermal cycling, these alloys exhibit stabilization of, or increases in, transformation temperatures with aging.
- These alloys can be processed into such bulk forms as bar, rod, sheet, plate, and wire through conventional thermomechanical processes. Because these alloys have high recrystallization temperatures (700 to 800 °C), they are amenable to heat treatment and aging after thermomechanical processing, without adversely affecting grain sizes.
- The high recrystallization temperatures also make these alloys suitable for use in applications in which they could be subjected to significant heating above their rated temperatures.

*This work was done by Ronald D. Noebe, Susan L. Draper, and Michael V. Nathal of Glenn Research Center and Edwin A. Crombie of Johnson Matthey, Noble Metal Products N.A. Further information is contained in a TSP (see page 1).*

*Inquiries concerning rights for the commercial use of this invention should be addressed to NASA Glenn Research Center, Innovative Partnerships Office, Attn: Steve Fedor, Mail Stop 4-8, 21000 Brookpark Road, Cleveland, Ohio 44135. Refer to LEW-17993-1.*





## Improved Relief Valve Would Be Less Susceptible to Failure

Opening force and, hence, opening piston speed would be reduced.

*Stennis Space Center, Mississippi*

The balanced-piston relief valve with side vented reaction cavity has been proposed as an improved alternative to a conventional high-pressure, high-flow relief valve. As explained below, the proposed valve would be less susceptible to failure.

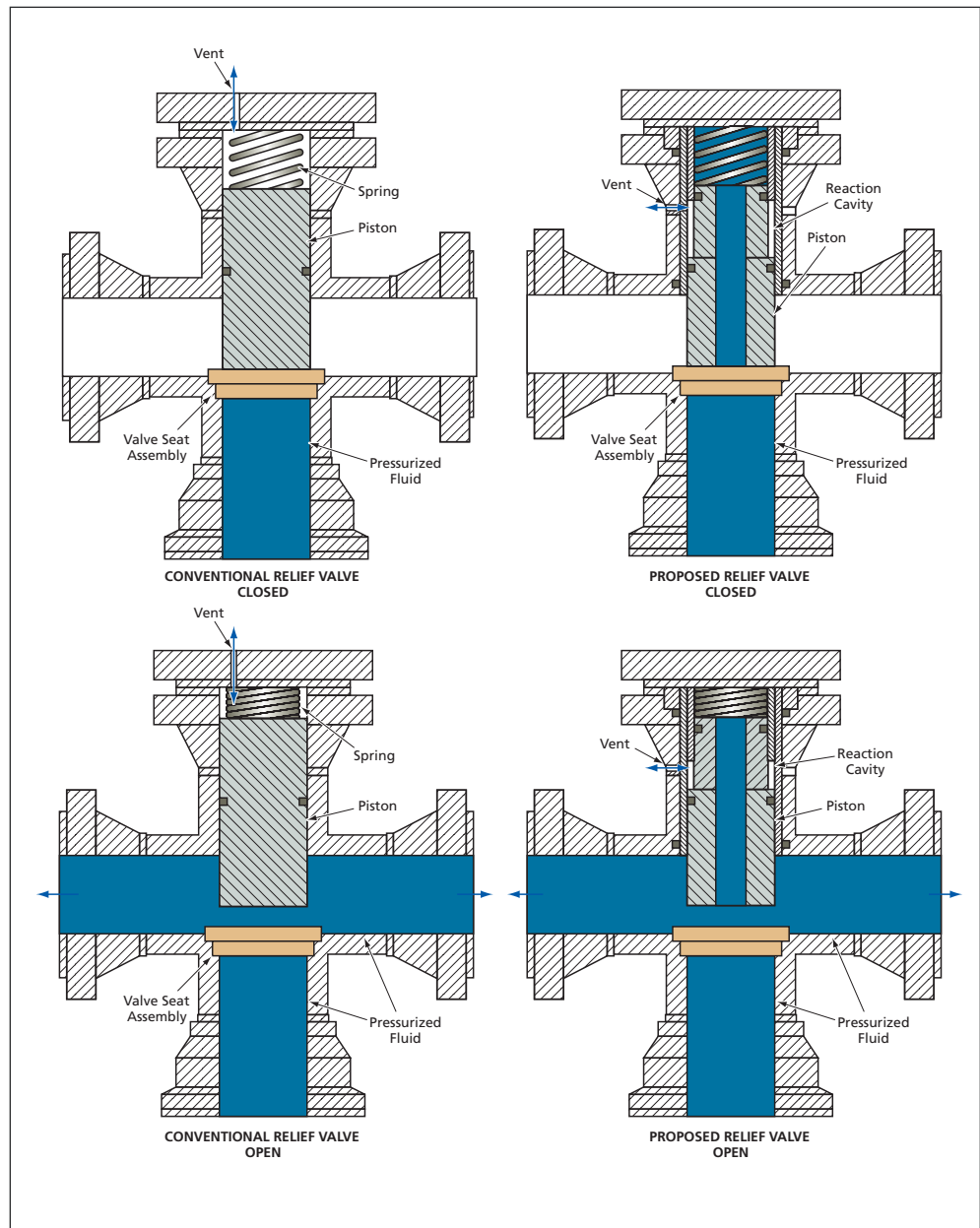
The left side of the figure shows a typical conventional high-pressure, high-flow relief valve, which contains a piston that is exposed to the upstream pressure across the full valve-seat diameter and is held against the valve seat and the upstream pressure by a large spring. In the event of an increase in upstream pressure to a level above the valve set point (the pressure above which the valve opens), the opening force on the piston can be so large that the piston becomes accelerated to a speed high enough that the ensuing hard impact of the piston within the valve housing results in failure of the valve.

For a given flow cross section, the proposal would significantly reduce the force, thereby reducing susceptibility to failure. A basic version of the proposed balanced-piston relief valve with side vented reaction cavity is depicted on the right side of the figure. The piston would contain a central hollow that would allow the pressurized fluid to flow into the spring cavity above the piston, so that the pressure in the fluid would act against both the upper and lower piston faces.

The outer diameter of the piston at the upper end would be somewhat less than the outer diameter of the piston at the lower end, the two diameters meeting at a shoulder on the side of the piston. A sleeve filling the annular space between the two diameters would surround the upper end of the piston. Therefore, the upper

piston face would be slightly smaller than the lower piston face, the difference between the areas of these faces being equal to the annular cross-sectional area of the sleeve or, equivalently, of the shoulder.

The reaction cavity (the annular side volume between the shoulder and the sleeve) would be vented to either the atmosphere or other source of reference pressure below the valve set point. As a result, the upward (opening) fluid pressure



In the **Proposed Relief Valve**, the net fluid-pressure opening force on the piston would be much less than in the conventional relief valve because the upward force of the fluid pressure on the bottom piston surface would be mostly counteracted by the downward force of the fluid pressure on the top piston surface.

force on the piston would exceed the downward (closing) fluid pressure force on the piston, the net upward fluid pressure force being equal to the annular area of the shoulder and the gauge pressure (absolute fluid pressure less atmospheric or other reference pressure). Because the annular shoulder area could be made less than the area of the lower piston face, the opening force could be tailored to a suit-

ably low value through design choice of the upper and lower piston diameters. (Of course, for a given valve set point, it would be necessary to choose a spring of correspondingly reduced stiffness.) The fluid in the spring cavity would present inertial impedance that would further reduce the opening acceleration of the piston. As an additional benefit, it may be possible to reseal the valve at a greater

fraction (perhaps as much as 100 percent) of the valve set point than that of a conventional relief valve.

*This work was done by Bruce R. Farner of Stennis Space Center.*

*Inquiries concerning rights for the commercial use of this invention should be addressed to the Intellectual Property Manager, Stennis Space Center, (228) 688-1929. Refer to SSC-00232-1.*

---

## Safety Modification of Cam-and-Groove Hose Coupling

**Coupling halves cannot be separated while the hose is internally pressurized.**

*John F. Kennedy Space Center, Florida*

A modification has been made in the mating halves of a cam-and-groove hose coupling to prevent rapid separation of the halves in the event that the cam levers are released while the fluid in the hose is pressurized. This modification can be duplicated on almost any commercially available cam-and-groove hose-coupling halves and does not interfere with most vendors' locks that prevent accidental actuation of the cam levers.

The need for this modification arises because commercial off-the-shelf cam-and-groove hose-coupling halves do not incorporate safety features to prevent separation in the pressurized state. Especially when the pressurized fluid is compressible (e.g., steam or compressed air), the separated halves can be propelled with considerable energy, causing personal injury and/or property damage. Therefore, one purpose served by the modification is to provide for venting to release compressive energy in a

contained and safe manner while preventing personal injury and/or property damage. Another purpose served by the modification, during the process of connecting the coupling halves, is to ensure that the coupling halves are properly aligned before the cam levers can be locked into position.

For the purpose of describing the modification, the coupling halves are denoted the receiving and mating halves, respectively. The modification includes the formation of two installation/removal slots and two safety pockets in the receiving coupling half. Each safety pocket is located at an angle of 45° from an installation/removal slot and provides both a "catch" to prevent accidental release and a landing for full installation. The mating coupling half has been modified to receive two shoulder bolts made of A286 stainless steel.

In use, if the mating coupling half is not rotated 1/8 turn relative to the re-

ceiving coupling half, then the cam levers cannot be rotated into position and locked to provide the required seal between the two coupling halves. The head of each shoulder bolt slides in one of the installation/removal slots and provides a stop if release is initiated accidentally while the fluid in the hose is pressurized. The safety pocket prevents rotation of the mating coupling half relative to the receiving coupling half while the fluid is pressurized, thereby also preventing sudden separation of the coupling halves. At the same time, the modifications allow the coupling halves to disengage slightly to allow venting of the pressurized fluid. Once pressure in the hose is sufficiently low, the coupling halves can be safely disconnected from each other.

*This work was done by Paul Schwindt and Alan Littlefield of Kennedy Space Center. Further information is contained in a TSP (see page 1), KSC-12713*

---

## Using Composite Materials in a Cryogenic Pump

**Shaft speed is increased and conductive leakage of heat is reduced.**

*John F. Kennedy Space Center, Florida*

Several modifications have been made to the design and operation of an extended-shaft cryogenic pump to increase the efficiency of pumping. In general, the efficiency of pumping a cryogenic fluid is limited by thermal losses (the thermal energy that the pump adds to the fluid). The sources of the thermal losses are pump inefficiency and leakage (conduction) of heat through the pump structure. Most cryogenic pumping systems are required to operate at maximum efficiency because

the thermal energy added to the fluids by the pumps is removed by expensive downstream refrigeration equipment. It would be beneficial to reduce thermal losses to the point where the downstream refrigeration equipment would not be necessary.

A typical cryogenic pump includes a drive shaft and two main concentric static components (an outer pressure containment tube and an intermediate static support tube) made from stainless steel. In order to reduce the leakage of heat, the

shaft is made longer than would otherwise be needed. The efficiency of the pump could be increased most easily by increasing the speed of rotation of the shaft, but the speed must be kept below the lowest of the rotordynamic critical speeds. (In essence, the rotordynamic critical speeds are resonance frequencies at which the interaction of rotational dynamics and elasticity of the shaft and the rest of the rotor can cause the rotor to vibrate uncontrollably, possibly damaging the pump.)

The modifications include replacement of the stainless-steel drive shaft and the concentric static stainless-steel components with components made of a glass/epoxy composite. The leakage of heat is thus reduced because the thermal conductivity of the composite is an order of magnitude below that of stainless steel. Taking advantage of the margin afforded by the decrease in thermal conductivity, the drive shaft could be shortened to increase its effective stiffness, thereby increasing the rotordynamic critical speeds, thereby further making it possible to operate the pump at a higher speed to increase pumping efficiency.

During the modification effort, an analysis revealed that substitution of the shorter glass/epoxy shaft for the longer stainless-steel shaft was not, by itself, sufficient to satisfy the rotordynamic requirements at the desired increased speed. Hence, it became necessary to increase the stiffness of the composite shaft. This stiffening was accomplished by means of a carbon-fiber-composite overwrap along most of the length of the shaft. Because the thermal conductivity of the carbon-fiber composite exceeds that of the glass-epoxy composite, it was necessary to choose the thickness

of the overwrap as a compromise between adequate stiffening and a need to minimize leakage of heat along the shaft. It was found to be possible to choose a compromise thickness [0.020 in. ( $\approx 0.5$  mm)] to satisfy the heat-leakage requirement while stiffening the shaft by a factor  $>10$  and thereby satisfying the rotordynamic requirements.

Concomitantly with the modifications described thus far, it was necessary to provide for joining the composite-material components with metallic components required by different aspects of the pump design. The metal/composite joints are required to withstand differential thermal contraction and expansion between ambient and cryogenic temperatures and to withstand torque and piping loads while maintaining a vacuum seal throughout the ambient-to-cryogenic temperature range. The joints are also required to have reasonable dimensional tolerances, to be easy to assemble in a repeatable process, and otherwise generally to be manufacturable at a level of effort and cost equivalent to that of the prior stainless-steel design.

An adhesive material formulated specially to bond the composite and metal components was chosen as a means to

satisfy these requirements. The particular adhesive material has a history of excellent performance in cryogenic applications. The joints were designed to put all the loading in shear and reduce stress concentrations. The joint design was optimized with respect to bond thickness, preparation of surfaces to be bonded, and the viscosity of the adhesive itself. A finite-element analysis predicted that the joints would satisfy the load-bearing requirements. Some mechanical tests verified that the joints could withstand the most severe loads imposed. (The loads were chosen, in part, to simulate the temperatures to be encountered in operation.) Other mechanical tests (tensile tests) demonstrated a factor of safety of 6 with respect to anticipated loads. Results of helium testing lent credence to the expectation that joints will not leak during operation.

*This work was done by William D. Batton, James E. Dillard, and Matthew E. Rottmund of Barber-Nichols, Inc.; and Michael L. Tupper, Kaushik Mallick, and William H. Francis of Composite Technology Development, Inc. for Kennedy Space Center. For further information, contact the Kennedy Innovative Partnerships Office at (321) 861-7158. KSC-12625/6/7*





## Using Electronic Noses To Detect Tumors During Neurosurgery

Sensors would help surgeons determine whether tumors have been removed completely.

NASA's Jet Propulsion Laboratory, Pasadena, California

It has been proposed to develop special-purpose electronic noses and algorithms for processing the digitized outputs of the electronic noses for determining whether tissue exposed during neurosurgery is cancerous. At

present, visual inspection by a surgeon is the only available intraoperative technique for detecting cancerous tissue. Implementation of the proposal would help to satisfy a desire, expressed by some neurosurgeons, for an intraopera-

tive technique for determining whether all of a brain tumor has been removed. The electronic-nose technique could complement multimodal imaging techniques, which have also been proposed as means of detecting cancerous tissue.

There are also other potential applications of the electronic-nose technique in general diagnosis of abnormal tissue.

In preliminary experiments performed to assess the viability of the proposal, the problem of distinguishing between different types of cultured cells was substituted for the problem of distinguishing between normal and abnormal specimens of the same type of tissue. The figure presents data from one experiment, illustrating differences between patterns that could be used to distinguish between two types of cultured cancer cells. Further development can be expected to include studies directed toward answering questions concerning not only the possibility of distinguishing among various types of normal and abnormal tissue but also distinguishing between tissues of interest and other odorous substances that may be present in medical settings.

*This work was done by Margie L. Homer and Margaret A. Ryan of Caltech, Liana M. Lara of Santa Barbara Research, and Babak Kateb and Mike Chen of City of Hope Medical Center for NASA's Jet Propulsion Laboratory. Further information is contained in a TSP (see page 1).*

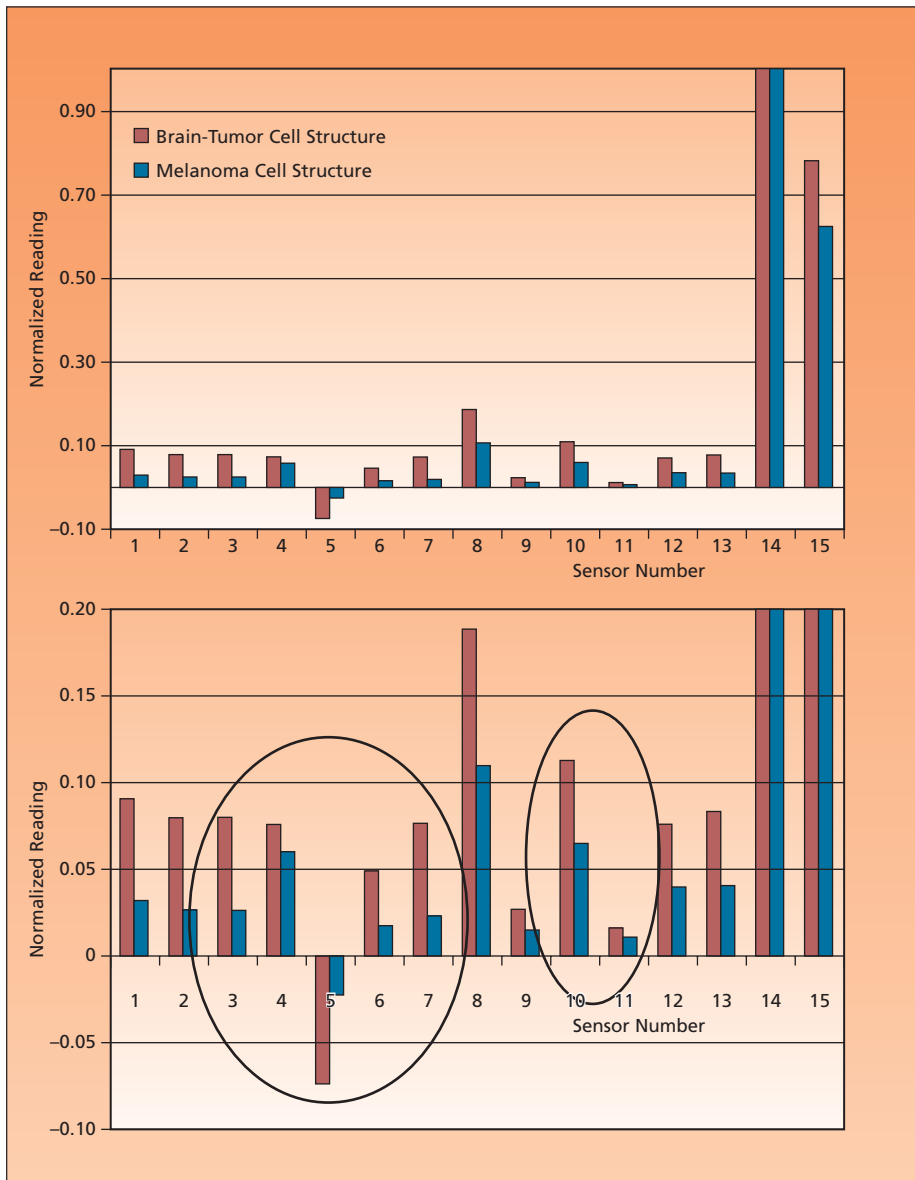
*In accordance with Public Law 96-517, the contractor has elected to retain title to this invention. Inquiries concerning rights for its commercial use should be addressed to:*

*Innovative Technology Assets Management  
JPL*

*Mail Stop 202-233  
4800 Oak Grove Drive  
Pasadena, CA 91109-8099*

*E-mail: iaoffice@jpl.nasa.gov*

*Refer to NPO-45433, volume and number of this NASA Tech Briefs issue, and the page number.*



**Processed Readings of the Sensors** in a 15-sensor electronic nose were recorded during an exposure to a melanoma cell culture and a brain-tumor cell culture. In processing the readings for each culture, growth-medium contributions were subtracted and all the readings were normalized to the largest reading. The lower plot is a vertically expanded version of the upper plot. In the regions enclosed by the ellipses, the differences between the patterns are considered to be typical of differences that would be sufficient to enable distinction between the two cell cultures.

# Producing Newborn Synchronous Mammalian Cells

**This invention could be used to study aging and cancer.**

*Lyndon B. Johnson Space Center, Houston, Texas*

A method and bioreactor for the continuous production of synchronous (same age) population of mammalian cells have been invented. The invention involves the attachment and growth of cells on an adhesive-coated porous membrane immersed in a perfused liquid culture medium in a microgravity analog bioreactor. When cells attach to the surface divide, newborn cells are released into the flowing culture medium. The released cells, consisting of a uniform population of synchronous cells are then collected from the effluent culture medium. This invention could be of interest to researchers investigating the effects of the geneotoxic effects of the space environment (microgravity, radiation, chemicals, gases) and to pharmaceutical and biotechnology companies involved in research on aging and cancer, and in new drug development and testing.

The bioreactor includes a horizontal-axis rotating vessel. A screen inside the vessel supports the porous membrane on which the cells are grown. A central

fluid coupler contains an inlet and an outlet port with rotating seals for the circulation of the culture medium. During operation for the growth of cells, a peristaltic pump delivers the culture medium from an external reservoir to the input port. On its way from the inlet to the outlet port, the culture medium flows through the membrane, entraining newly released baby cells in the flow. Once the culture medium has flowed out of the simulated-low-gravity environment of the rotating vessel, the baby cells are collected by allowing them to settle out of the liquid under the influence of normal Earth gravitation.

Prior to operation for the growth of cells, the membrane is coated with a cell adhesive on the side designated to be downstream during operation of the bioreactor. This is done by filtering a solution of adhesive through it in the reverse of the operational flow direction. The membrane is then washed with a similarly reversed flow of water or a phosphate buffered saline solution. Next, growing cells are applied to the

downstream side of the membrane by means of a similarly reverse flow of a medium containing a cell culture. These reverse-flow operations for preparation of the membrane can take place either before or after the membrane is mounted in the vessel: If membrane is mounted in the vessel first, then the adhesive solution, wash solution, and culture medium are simply pumped through the vessel in the reverse of the operational flow direction.

*This work was done by Steve R. Gonda of Johnson Space Center and Charles E. Helmstetter and Maureen Thornton of Florida Institute of Technology. Further information is contained in a TSP (see page 1).*

*In accordance with Public Law 96-517, the contractor has elected to retain title to this invention. Inquiries concerning rights for its commercial use should be addressed to:*

*Florida Institute of Technology:*

*150 W University Blvd.*

*Melbourne, FL 32901*

*Refer to MSC-23476-1, volume and number of this NASA Tech Briefs issue, and the page number.*



## **Smaller, Lower-Power Fast-Neutron Scintillation Detectors**

**There are numerous potential applications in scientific and safety-oriented monitoring of fast neutrons.**

*NASA's Jet Propulsion Laboratory, Pasadena, California*

Scintillation-based fast-neutron detectors that are smaller and less power-hungry than mainstream scintillation-based fast-neutron detectors are undergoing development. There are numerous applications for such detectors in monitoring fast-neutron fluxes from nuclear reactors, nuclear materials, and natural sources, both on Earth and in outer space. A particularly important terrestrial application for small, low-power, portable fast-neutron detectors lies in the requirement to scan for nuclear materials in cargo and baggage arriving at international transportation facilities.

In the conventional method of detecting fast neutrons (by which is meant neutrons having kinetic energies greater than about 10 keV), the neutrons are first decelerated, by use of moderator materials (typically, paraffin or polyethylene) to near thermal kinetic energies, in order to exploit the fact that the cross sections for interactions of neutrons with other nuclei are largest at low kinetic energies. To be useful for this purpose, moderators must be several inches (of the order of 10 cm) thick. In addition, one must use gas-filled detector tubes containing electrodes to which high bias voltages are applied. Hence, conventional fast-neutron detectors are inherently bulky and heavy.

Several decades ago, scintillation-based detectors were introduced as smaller alternatives to conventional fast-neutron detectors. A scintillation detector of this type includes a photomultiplier tube that monitors a block of a scintillator material (typically, a crystal or a plastic containing a hydrogen rich scintillation dye). A scintillation pulse occurs when a fast neutron knocks a proton in the scintillation material and some of the kinetic energy of the decelerating proton excites luminescence. Although the use of a block of scintillator material is a step toward miniaturization, a photomultiplier tube is still a bulky, high-power device.

The present development of miniature, low-power scintillation-based fast-neutron detectors exploits recent advances in the fabrication of avalanche photodiodes (APDs). Basically, such a detector includes a plastic scintillator, typically between 300 and 400  $\mu\text{m}$  thick with very thin silver mirror coating on all its faces except the one bonded to an APD (see figure). All photons generated from scintillation are thus internally reflected and eventually directed to the APD. This design affords not only compactness but also tight optical coupling for utilization of a relatively large proportion of the scintillation light. The combination of

this tight coupling and the avalanche-multiplication gain (typically between 750 and 1,000) of the APD is expected to have enough sensitivity to enable monitoring of a fast-neutron flux as small as  $1,000 \text{ cm}^{-2}\text{s}^{-1}$ . Moreover, pulse-height analysis can be expected to provide information on the kinetic energies of incident neutrons. It has been estimated that a complete, fully developed fast-neutron detector of this type, would be characterized by linear dimensions of the order of 10 cm or less, a mass of no more than about 0.5 kg, and a power demand of no more than a few watts.

*This work was done by Jagdish Patel and Brent Blaes of Caltech for NASA's Jet Propulsion Laboratory. Further information is contained in a TSP (see page 1).*

*In accordance with Public Law 96-517, the contractor has elected to retain title to this invention. Inquiries concerning rights for its commercial use should be addressed to:*

*Innovative Technology Assets Management  
JPL*

*Mail Stop 202-233  
4800 Oak Grove Drive  
Pasadena, CA 91109-8099  
(818) 354-2240*

*E-mail: iaoffice@jpl.nasa.gov*

*Refer to NPO-41345, volume and number of this NASA Tech Briefs issue, and the page number.*

## **Rotationally Vibrating Electric-Field Mill**

**The disadvantages of rotary couplings in conventional field mills could be avoided.**

*NASA's Jet Propulsion Laboratory, Pasadena, California*

A proposed instrument for measuring a static electric field would be based partly on a conventional rotating-split-cylinder or rotating-split-sphere electric-field mill. However, the design of the proposed instrument would overcome the difficulty, encountered in conventional rotational field mills, of transferring measurement signals and power via either electrical or fiber-optic rotary couplings that must be

aligned and installed in conjunction with rotary bearings. Instead of being made to rotate in one direction at a steady speed as in a conventional rotational field mill, a split-cylinder or split-sphere electrode assembly in the proposed instrument would be set into rotational vibration like that of a metronome. The rotational vibration, synchronized with appropriate rapid electronic switching of electrical connections

between electric-current-measuring circuitry and the split-cylinder or split-sphere electrodes, would result in an electrical measurement effect equivalent to that of a conventional rotational field mill.

The figure depicts a version of the proposed instrument, the electrode assembly of which would include a hollow metal hemisphere split into four electrodes. Instead of a conventional rotary

bearing, the instrument would include a flexural bearing that would be part of a metronomelike actuator. The measurement-signal and power connections between the electrode assembly and external instrumentation would be made via optical fibers that would flex with the flexural bearing.

The flexural bearing and actuator would be anchored to a stationary base, on which data-acquisition and power-supply electronic circuits would be mounted. In addition to the electrodes, the electrode assembly would contain electronic circuits for switching the electrical connections to the electrodes,

measuring the electric currents that flow between connected electrodes as the assembly rotates in the ambient electric field, digitizing the current measurements, and transmitting the digitized measurement signals to the data-acquisition circuitry via one of the optical fibers. Power would be transmitted from a light-emitting diode on the stationary base, via another optical fiber, to photovoltaic circuitry in the electrode assembly.

Because the flexural bearing, its actuator, and the electrode assembly taken together would constitute a resonant mechanical system like a metronome, little

power would be needed to maintain the large angular excursions needed to produce sufficiently large measurement signals. The precise nature of the actuator has not yet been determined; it seems likely that a magnetic drive could easily be implemented. The actuator could be equipped with a rotary position encoder, which could provide feedback for adjusting the excitation of the actuator to correct for small deviations of the rotational vibration from constant frequency and amplitude.

*This work was done by Harold Kirkham of Caltech for NASA's Jet Propulsion Laboratory. Further information is contained in a TSP (see page 1). NPO-30572*

## Estimating Hardness From the USDC Tool-Bit Temperature Rise

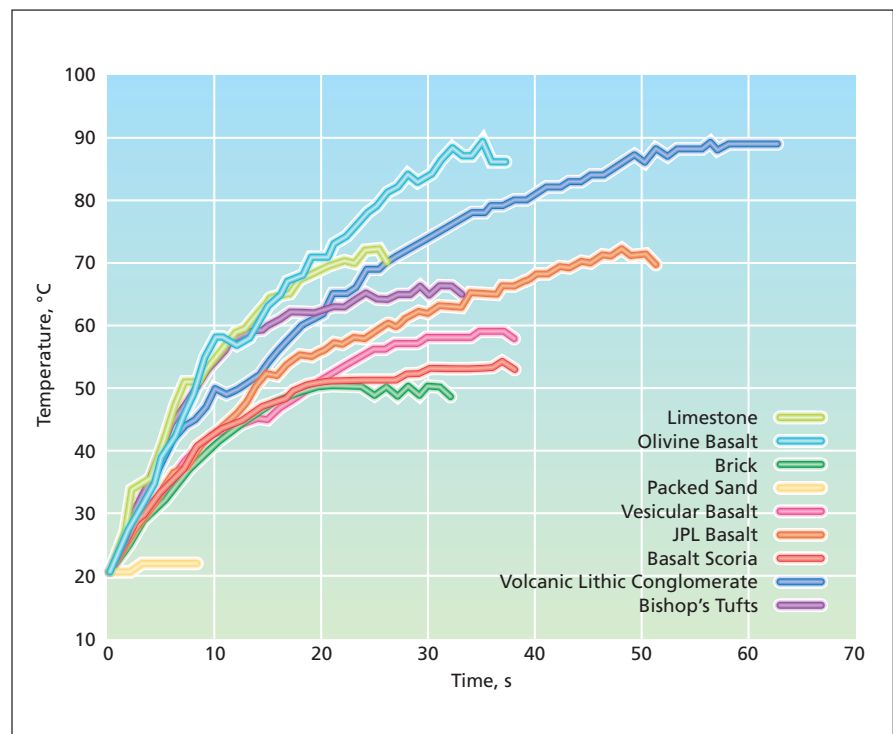
Temperature rise during drilling is correlated with hardness of the drilled material.

NASA's Jet Propulsion Laboratory, Pasadena, California

A method of real-time quantification of the hardness of a rock or similar material involves measurement of the temperature, as a function of time, of the tool bit of an ultrasonic/sonic drill corer (USDC) that is being used to drill into the material. The method is based on the idea that, other things being about equal, the rate of rise of temperature and the maximum temperature reached during drilling increase with the hardness of the drilled material.

In this method, the temperature is measured by means of a thermocouple embedded in the USDC tool bit near the drilling tip. [The concept of incorporating sensors into USDC tool bits was described in "Ultrasonic/Sonic Drill/Corers With Integrated Sensors" (NPO-20856), *NASA Tech Briefs*, Vol. 25, No. 1 (January 2001), page 38.] The hardness of the drilled material can then be determined through correlation of the temperature-rise-versus-time data with time-dependent temperature rises determined in finite-element simulations of, and/or experiments on, drilling at various known rates of advance or known power levels through materials of known hardness. The figure presents an example of empirical temperature-versus-time data for a particular 3.6-mm USDC bit, driven at an average power somewhat below 40 W, drilling through materials of various hardness levels.

The temperature readings from within a USDC tool bit can also be



Temperature-Versus-Time data were obtained by use of a thermocouple embedded near a USDC tool bit drilling through materials of various hardness levels.

used for purposes other than estimating the hardness of the drilled material. For example, they can be especially useful as feedback to control the driving power to prevent thermal damage to the drilled material, the drill bit, or both. In the case of drilling through ice, the temperature readings could be used as a guide to maintain-

ing sufficient drive power to prevent jamming of the drill by preventing re-freezing of melted ice in contact with the drill.

*This work was done by Yoseph Bar-Cohen and Stewart Sherrit of Caltech for NASA's Jet Propulsion Laboratory. For more information, contact iaoffice@jpl.nasa.gov. NPO-40132*



# Particle-Charge Spectrometer

A flow of gas carries charged particles through a charge-sensing cylindrical electrode.

NASA's Jet Propulsion Laboratory, Pasadena, California

An instrument for rapidly measuring the electric charges and sizes (from  $\approx 1$  to  $\approx 100 \mu\text{m}$ ) of airborne particles is undergoing development. Conceived for monitoring atmospheric dust particles on Mars, instruments like this one

could also be used on Earth to monitor natural and artificial aerosols in diverse indoor and outdoor settings — for example, volcanic regions, clean rooms, powder-processing machinery, and spray-coating facilities.

The instrument incorporates a commercially available, low-noise, ultrasensitive charge-sensing preamplifier circuit. The input terminal of this circuit — the gate of a field-effect transistor — is connected to a Faraday-cage cylindrical electrode. The charged particles of interest are suspended in air or other suitable gas that is made to flow along the axis of the cylindrical electrode without touching the electrode. The flow can be channeled and generated by any of several alternative means; in the prototype of this instrument, the gas is drawn along a glass capillary tube (see upper part of figure) coaxial with the electrode.

The size of a particle affects its rate of acceleration in the flow and thus affects the timing and shape of the corresponding signal peak generated by the charge-sensing amplifier. The charge affects the magnitude (and thus also the shape) of the signal peak. Thus, the signal peak (see figure) conveys information on both the size and electric charge of a sensed particle.

In experiments thus far, the instrument has been found to be capable of measuring individual aerosol particle charges of magnitude  $>350 e$  (where  $e$  is the fundamental unit of electric charge) with a precision of  $\pm 150 e$ . The instrument can sample particles at a rate as high as several thousand per second.

*This work was done by Stephen Fuerstenau and Gregory R. Wilson of Caltech for NASA's Jet Propulsion Laboratory.*

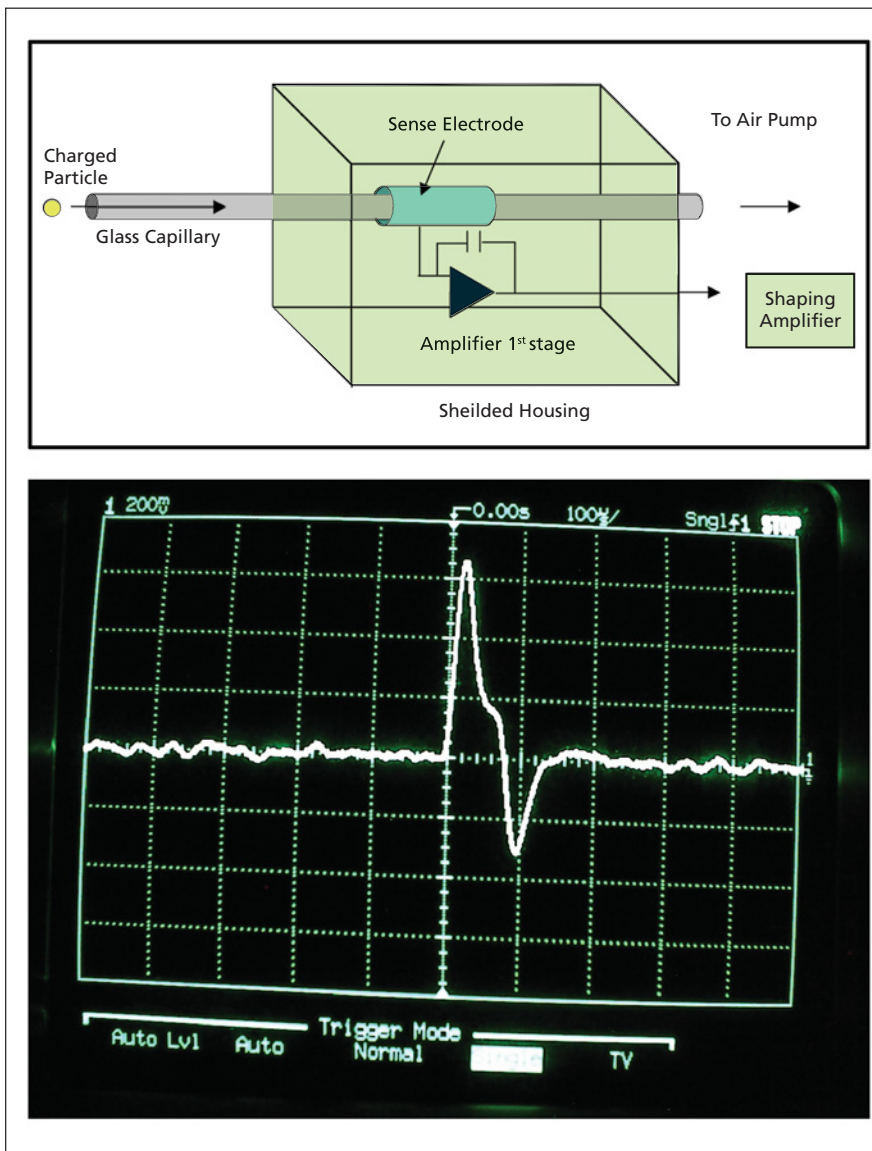
*In accordance with Public Law 96-517, the contractor has elected to retain title to this invention. Inquiries concerning rights for its commercial use should be addressed to:*

*Innovative Technology Assets Management  
JPL*

*Mail Stop 202-233  
4800 Oak Grove Drive  
Pasadena, CA 91109-8099*

*E-mail: iaoffice@jpl.nasa.gov*

*Refer to NPO-21183, volume and number of this NASA Tech Briefs issue, and the page number.*



The Prototype Particle-Charge Spectrometer includes a capillary tube that enters a shielded housing containing a Faraday-cage cylindrical electrode and charge-sensing electronic circuitry. The oscilloscope trace depicts the charge-sensing output signal in response to a particle of charge  $\approx 1,560 e$ .





## Automated Production of Movies on a Cluster of Computers

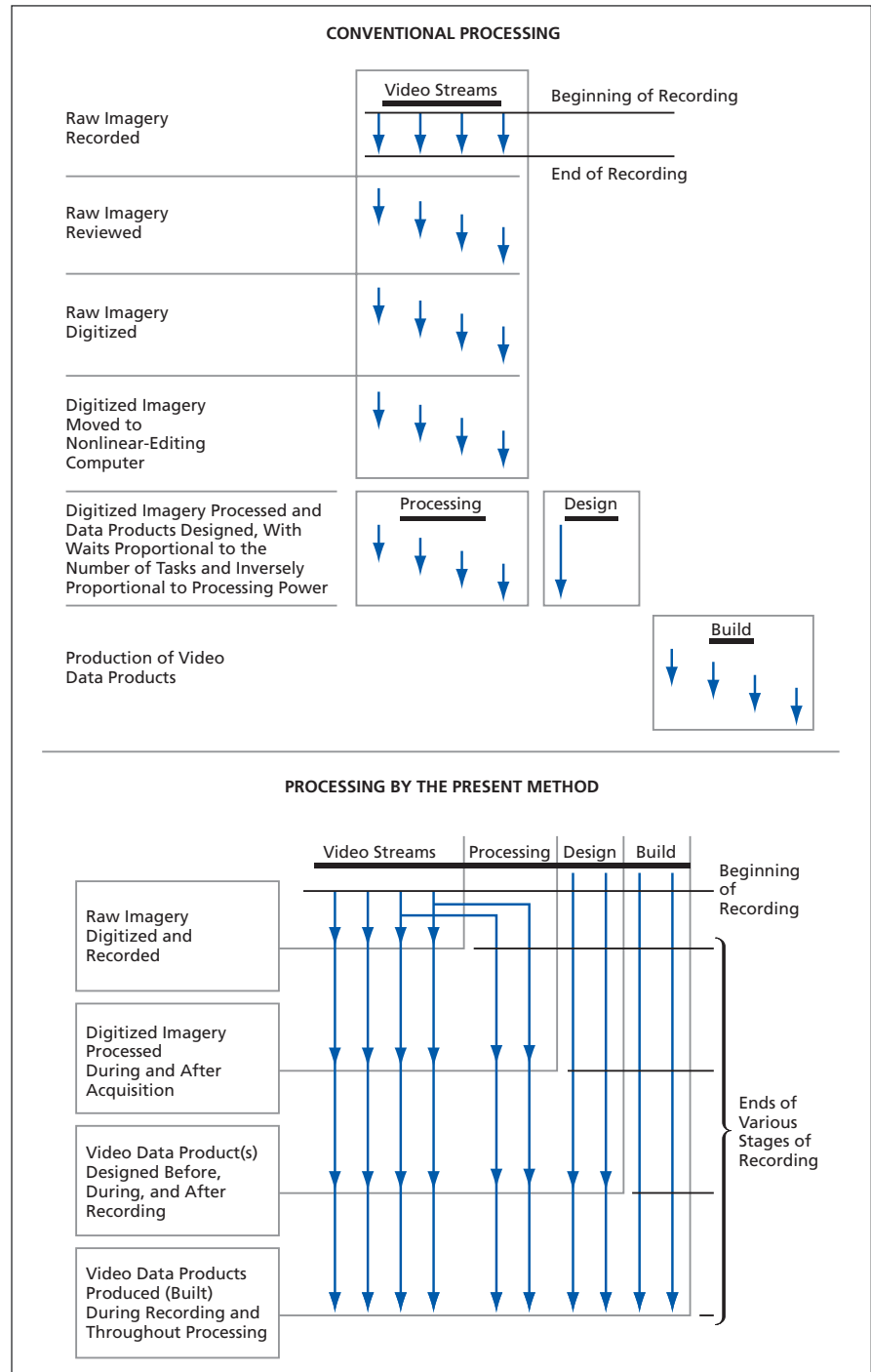
**Processing is faster, easier, more flexible, and more collaborative than before.**

*Stennis Space Center, Mississippi*

A method of accelerating and facilitating production of video and film motion-picture products, and software and generic designs of computer hardware to implement the method, are undergoing development. The method provides for automation of most of the tedious and repetitive tasks involved in editing and otherwise processing raw digitized imagery into final motion-picture products. The method was conceived to satisfy requirements, in industrial and scientific testing, for rapid processing of multiple streams of simultaneously captured raw video imagery into documentation in the form of edited video imagery and video derived data products for technical review and analysis. In the production of such video technical documentation, unlike in production of motion-picture products for entertainment, (1) it is often necessary to produce multiple video derived data products, (2) there are usually no second chances to repeat acquisition of raw imagery, (3) it is often desired to produce final products within minutes rather than hours, days, or months, and (4) consistency and quality, rather than aesthetics, are the primary criteria for judging the products.

In the conventional method of processing video imagery, the workflow is mostly serial in the sense that for the most part, each stage of processing must be completed before beginning the next stage, and the final product is a single video stream. In the present method, the workflow has both serial and parallel aspects: processing can begin before all the raw imagery has been acquired, each video stream can be subjected to different stages of processing simultaneously on different computers that may be grouped into one or more cluster(s), and the final product may consist of multiple video streams (see figure). Results of processing on different computers are shared, so that workers can collaborate effectively.

The software provides a platform-independent design format, enabling pro-



**Workflow in Processing of Video Imagery** is substantially serial in the conventional method but has both parallel and serial character in the present method.

duction on a cluster of diverse shared and/or dedicated processors. The software generates a graphical user interface (GUI) for designing automatic production of dynamic video and film products. The GUI includes a visual programming language that uses interactive computer-graphical versions of constructs (e.g., story boards) familiar to professionals in the motion-picture industry. The software provides for the use of programming techniques that do not rely on the availability of raw video imagery or of certain dependent and inde-

pendent variables at the time of design. These programming techniques apply to editing, compositing, and rendering processes. The software enables production of a variety of products from a single design, partly through reuse of design elements and programmable features. The software enables automatic alterations of the product(s) during production to meet certain design goals. These automatic production changes can be based on the characteristics of the raw video imagery and of other variables as they become available.

*This work was done by Jasper Nail, Duong Le, William L. Nail, and William "Bud" Nail of Technological Services Co. for Stennis Space Center. Inquiries concerning rights for its commercial use should be addressed to:*

*Technological Services Company*

*P.O. Box 1218*

*100 Street A, Suite B*

*Picayune, MS 39466*

*Telephone No. (601) 799-2403*

*E-mail: budnail@videocomp.com.*

*Refer to SSC-00238, volume and number of this NASA Tech Briefs issue, and the page number.*



## Books & Reports

### **FIDO-Class Development Rover**

A report describes a rover-type robotic wheeled vehicle recently built for use as a testbed for development of software for future rover-type vehicles. This vehicle is a derivative of the Field Integrated Design and Operations (FIDO) rover, which is a prototype Mars-exploration rover that also serves as a terrestrial testbed.

The present vehicle was designed to be nearly functionally identical to the FIDO rover but to be built at much lower cost and to incorporate several improvements to increase utility for development work. Accordingly, considerable effort was made to use commercial off-the-shelf parts and other parts that could be fabricated easily and at low cost. Important features of this vehicle include six-wheel drive and six-wheel steering; onboard computer and power, control, and data-communication electronics having flexibility needed for development of software; significantly increased maximum speed (60 cm/s versus 6 cm/s for the

FIDO rover); a rocker-bogey suspension with external differential link, functionally equivalent to that of the FIDO rover; and a hand-held remote controller that can be used to control vehicle motion manually without using the computer (or while waiting for the onboard computer to boot up).

*This work was done by Herman Herman and Reid Simmons of Carnegie Mellon University and Richard D. Petras of Caltech for NASA's Jet Propulsion Laboratory. Further information is contained in a TSP (see page 1). NPO-45645*

### **Tone-Based Command of Deep Space Probes Using Ground Antennas**

A document discusses a technique for enabling the reception of spacecraft commands at received signal levels as much as three orders of magnitude below those of current deep space systems. Tone-based commanding deals with the reception of commands that are sent in the form of precise frequency offsets using an open-loop receiver. The

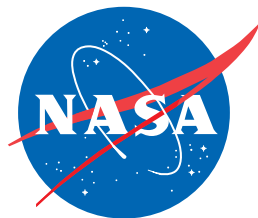
key elements of this technique are an ultrastable oscillator and open-loop receiver onboard the spacecraft, both of which are part of the existing New Horizons (Pluto flyby) communications system design. This enables possible flight experimentation for tone-based commanding during the long cruise of the spacecraft to Pluto.

In this technique, it is also necessary to accurately remove Doppler shift from the uplink signal presented to the spacecraft. A signal processor in the spacecraft performs a discrete Fourier transform on the received signal to determine the frequency of the received signal. Due to the long-term drift in the oscillators and orbit prediction model, the system is likely to be implemented differentially, where changes in the uplink frequency convey the command information.

*This work was done by Robert S. Bokulic and J. Robert Jensen of Johns Hopkins University Applied Physics Laboratory for Goddard Space Flight Center. Further information is contained in a TSP (see page 1). GSC-14966-1*







National Aeronautics and  
Space Administration